

國立臺灣大學理學院海洋研究所



碩士論文

Institute of Oceanography

College of Science

National Taiwan University

Master Thesis

以系集預測探討氣候變遷對南太平洋長鰭鮪分布之影響

Evaluation of the impacts of climate change on albacore

distribution in the South Pacific Ocean by using

ensemble forecast

賴柏凱

Po-Kai Lai

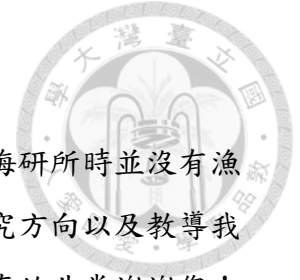
指導教授：張以杰 博士

Advisor: Yi-Jay Chang, Ph.D.

中華民國 109 年 7 月

July, 2020

謝辭



首先要感謝張以杰老師這兩年來的耐心指導，還記得剛進入海研所時並沒有漁業相關背景，對於做研究也沒什麼概念，幸好老師提供我論文研究方向以及教導我做研究的精神，讓我從無到有完成這篇千錘百鍊的論文，這兩年真的非常謝謝您！覺得老師雖然對於研究品質的要求高，但私底下是個蠻好相處的人，每次聽老師講自己的故事都覺得非常精彩，希望之後有機會可以再一起去衝浪或潛水。

再來要感謝研究室的大家，謝謝許蓁學姐陪我腦力激盪解決各種難題，尤其是最後幾個月水深火熱的時候多虧有妳不計辛勞的幫忙，還有平時打點研究室的大小事。偉哲在這一年之中也給了我許多幫助，不管是平常下午的外出散心還是提供專業現釣的海鮮，你真的是我在學校的好夥伴。還有以前畢業的學長們跟新進的學弟妹，緒邦、坤佑、哲越、資評，很幸運能在這段時間認識你們，雖然只是短短的兩年但已經留下數不清的回憶。謝謝海研所的同學們，我們一起度過了兩年的碩班生活，祝你們未來發展順利。特別感謝我的好兄弟，思維，從大學到研究所展不斷的孽緣，你都變成我們研究室的隱藏人物了，未來還要請你多多關照。還要感謝臺大羽球隊的隊友們，雖然一起練球的時間不長，但球隊永遠是我的另一個歸屬。謝謝晏琪，在碩班忙碌的生活裡我們總是陪在彼此身邊，現在也終於一起畢業了。

最後要感謝我的家人，謝謝你們支持我繼續念研究所，並且提供生活上的支援，讓我可以沒有後顧之憂的完成我的學業。要感謝的人真的太多，謝謝一路上走來身邊的每一個人，在此跟你們分享完成論文的喜悅。

賴柏凱

2020.8.12

Table of contents



摘要	i
Abstract	ii
Chapter 1 Introduction	1
1.1 <i>Albacore tuna biology</i>	1
1.2 <i>Albacore tuna fisheries</i>	2
1.3 <i>The impact of environmental variability and climate change</i>	3
1.4 <i>Objectives</i>	4
Chapter 2 Materials and Methods	6
2.1 <i>Fishery data</i>	6
2.2 <i>Historical and future environmental data</i>	7
2.3 <i>Species distribution model</i>	8
2.4 <i>Historical and future albacore distribution projection</i>	9
2.5 <i>Ensemble forecasting</i>	10
2.6 <i>Expected changes in EEZs</i>	11
Chapter 3 Results	12
3.1 <i>Albacore distribution model</i>	12
3.2 <i>Albacore distribution in the historical fishing period</i>	13
3.3 <i>Future projections</i>	14
Chapter 4 Discussion	18
References	23
Tables	30
Figures	35
Appendix Figures	48

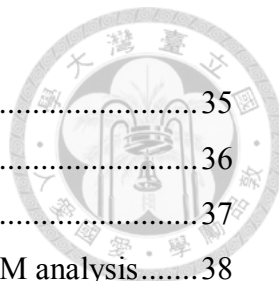
List of tables

Table 1. Summary of the flags of longline fleets	30
Table 2. List of atmosphere-ocean general circulation models.....	31
Table 3. Model and variable selection for the GAM.....	32
Table 4. Percentage changes in residual deviance and Akaike information criterion value of dropping each factor from the GAM.....	33
Table 5. Model performance measured by five-fold cross-validation.....	34

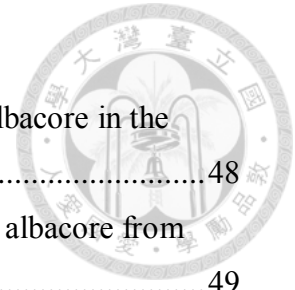


List of figures

Figure 1. Boxplot of catch-per-unit-effort by flags.....	35
Figure 2. Pairwise scatter plots of the environmental variables	36
Figure 3. Residual diagnostics of the GAM analysis	37
Figure 4. Response curves for the environmental variables from the GAM analysis.....	38
Figure 5. Response plots for the fixed factors from the GAM analysis	39
Figure 6. Quarterly average catch-per-unit-effort distributions overlaid on the median-ensemble density map from the GAM analysis	40
Figure 7. Time-series of the areal-averaged environmental variables (2020 to 2080) derived from IPCC atmosphere-ocean general circulation models.....	41
Figure 8. Spatial distributions of the albacore density predicted by different atmosphere-ocean general circulation models	42
Figure 9. Ensemble projections of albacore distribution in future periods.	43
Figure 10. Spatial distributions of albacore density anomalies in future periods	44
Figure 11. Ensemble agreement maps of albacore preferred habitats.....	45
Figure 12. Spatial distributions of uncertainty of predicted density in future periods.....	46
Figure 13. Changes in albacore density within the exclusive economic zones	47

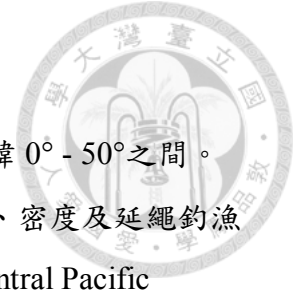


List of Appendices



Appendix figure 1. Map of schematic seasonal migration route of the albacore in the Western and Central Pacific Ocean	48
Appendix figure 2. Time-series of total annual catches of South Pacific albacore from 1952 to 2018.	49
Appendix figure 3. Spatial distribution of south Pacific albacore catches during 1988 - 2018.	50
Appendix figure 4. Spatial distributions of uncertainty of projected chlorophyll-a concentration in future periods	51
Appendix figure 5. Spatial distributions of uncertainty of projected sea surface temperature in future periods	52
Appendix figure 6. Spatial distributions of uncertainty of projected sea surface salinity in future periods	53
Appendix figure 7. Spatial distributions of uncertainty of projected mixed layer depth in future periods	54
Appendix figure 8. Spatial distributions of uncertainty of projected dissolved oxygen concentration in future periods	55
Appendix figure 9. Annual catch-per-unit-effort distributions overlaid on the median-ensemble density map in 1997 - 2006 based on the GAM analysis.....	56
Appendix figure 10. Annual catch-per-unit-effort distributions overlaid on the median-ensemble density map in 2007 - 2016 based on the GAM analysis.....	57
Appendix figure 11. Maps of the median ensemble predictions of sea surface temperature in future periods	58
Appendix figure 12. Maps of the median ensemble predictions of sea surface salinity in future periods	59
Appendix figure 13. Maps of the median ensemble predictions of mixed layer depth in future periods	60
Appendix figure 14. Maps of the median ensemble predictions of dissolved oxygen concentration in future periods	61

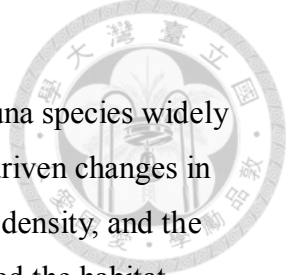
摘要



南太平洋長鰭鮪為高度洄游性魚種，廣泛分佈於南太平洋南緯 0° - 50° 之間。氣候變遷所導致的海洋環境變異會顯著影響南太平洋長鰭鮪分布、密度及延繩釣漁業之利用度。本研究蒐集中西太平洋漁業委員會 (Western and Central Pacific Fisheries Commission, WCPFC) 及美洲熱帶鮪魚委員會 (Inter-American Tropical Tuna Commission, IATTC) 延繩釣漁業資料以泛加成模型探討南太平洋長鰭鮪之空間分佈和棲地偏好。此外，本研究考慮各種大氣-氣候系統模式及碳排放情境 (RCP4.5 和 RCP8.5) 之氣候變遷下環境條件以系集預測降低長鰭鮪未來分布預測 (2020, 2050 及 2080 年) 之不確定性。結果顯示海下 100 公尺溶氧量及海表面溫度對長鰭鮪潛在分佈之影響最為重要，長鰭鮪偏好海下 100 公尺溶氧量介於 $0.2 - 0.25 \text{ mmol L}^{-1}$ 及海表面溫度介於 $13 - 22^{\circ}\text{C}$ 之棲地。本研究顯示在兩種 RCP 情境下，未來南太平洋長鰭鮪偏好棲地範圍之北界可能會南移約 5° 緯度，而在南緯 30° 以南海域之長鰭鮪密度則會增加，且該變動在 RCP8.5 情境下更為明顯。此外，本研究預測 2080 年長鰭鮪密度於南太平洋大部分國家之經濟水域可能有減少現象，其中以新喀里多尼亞減少的程度最高；然而在紐西蘭及諾福克島經濟水域之長鰭鮪密度則會增加。這些發現可作為氣候變遷下鮪類漁業利用度及其養護管理措施評估之漁業管理意涵。

關鍵字: 南太平洋長鰭鮪、系集預測、氣候變遷、物種分布模式

Abstract



South Pacific albacore (*Thunnus alalunga*) is a highly migratory tuna species widely distributed throughout 0° to 50°S in the South Pacific Ocean. Climate-driven changes in the oceanographic condition largely influence the albacore distribution, density, and the consequent availability by the longline fisheries. In this study, I examined the habitat preference and spatial distribution of south Pacific albacore using a generalized additive model fitted to the longline fisheries data from the Western and Central Pacific Fisheries Commission (WCPFC) and Inter-American Tropical Tuna Commission (IATTC). Future projections of albacore distributions (2020, 2050, and 2080) were predicted by using an ensemble modelling approach produced from various atmosphere-ocean general circulation models and anthropogenic emission scenarios (i.e., RCP4.5 and RCP8.5) to reduce the uncertainty in the projected changes. The dissolved oxygen concentration at 100 meters (DO100) and sea surface temperature (SST) were found to have the most substantial effects on the potential albacore distribution that the albacore preferred in the habitat with DO100 of 0.2 - 0.25 mmol L⁻¹ and SST of 13 - 22 °C. This study suggested that the northern boundary of albacore preferred habitat is expected to shift southward by about 5° latitudes, and the density is expected to gradually increase in the area south of 30°S from 2020 to 2080 for both RCP scenarios, especially with a higher degree of change for the RCP8.5. Moreover, the albacore density is projected to decrease in the most exclusive economic zones (EEZs) of countries and territories in the South Pacific Ocean by 2080 with the greatest depletion for New Caledonia, but is projected to increase in the EEZs of New Zealand and Norfolk Island. These findings could lend important implications on the availability of tuna resources to the fisheries and subsequent evaluation of tuna conservation and management measures under climate change.

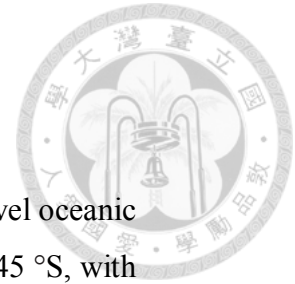
Keywords: South Pacific albacore, ensemble forecasting, climate change, species distribution model

Chapter 1 Introduction

1.1 *Albacore tuna biology*

Albacore tuna (*Thunnus alalunga*) is an important upper tropic-level oceanic predator which distributed globally between approximately 50 °N and 45 °S, with relatively lower abundance in equatorial areas. Albacore is a moderate-sized tuna with a maximum reported size of 127 cm fork length (FL) and 40 kg, with remarkably long pectoral fins that reaching beyond the origin of second dorsal fin (Collette and Nauen, 1983). Growth is rapid in early life, the first age class recruit in the fisheries in a size range of 45 - 50 cm FL (Leroy and Lehodey, 2004), mature at around 87 cm FL and 4.5 years (Farley et al., 2014), most of the fish live for more than 10 years. They inhabit in mesopelagic waters and mainly feed on small crustaceans and fishes such as krill and mackerel (Glaser et al., 2015; Williams et al., 2015), preferred lower water temperature between 15.6 to 19.4 °C. There are two stocks of albacore in the Pacific Ocean, one in the northern hemisphere and the other in the southern hemisphere (Arrizabalaga et al., 2004) where they show similar latitudinal distribution and seasonal migration pattern (Langley and Hampton, 2005; Childers et al., 2011).

In the south Pacific Ocean, the mature albacore (> 80 cm FL) migrates to spawning ground and spawns in the Coral Sea during late spring and early summer, November - February (Ramon and Bailey, 1996), juveniles (< 80 cm FL) are recruited to surface coastal waters off New Zealand to feed on preys. About one year later, juveniles then disperse northwards from the Subtropical Convergence Zone (STCZ, at about 40 °S) (**Appendix Figure 1**) and migrate seasonally between tropical and sub-tropical waters following 23 - 28 °C sea surface temperature band (Hoyle et al., 2012), with movement toward southern area during early summer and northward movement during winter (Langley and Hampton, 2005). Juvenile albacore typically occurs along oceanic fronts in surface waters, mainly feed on micronekton, whereas adults are found in deeper water, feed primarily on squid, sardines, and mackerels. Albacores in the tropics feed on more deep-water prey, compared to fish in temperate areas where they mainly consume



crustaceans (Williams et al., 2015).

1.2 *Albacore tuna fisheries*

Albacore is a commercially important species that are considered as one of the best types of tuna available for canning (Gloria et al., 1999) and contributed about 4% to the annual global tuna catch of 7.5 million tons in 2018 (FAO, 2018). Most of the world's catch of albacore tuna (65%) is taken in the Pacific Ocean (FAO, 2018). One of the largest fisheries for albacore is in the South Pacific Ocean where annual harvest contributed about 60% of the catch in the Pacific. In the South Pacific Ocean, most of the albacore was taken by longline fisheries (> 90%), especially for distant water longline fishing vessels from Taiwan, China, and the domestic longline fleets of various Pacific Island countries and territories (PICTs) (Brouwer et al., 2018). Total catch has fluctuated around 80,000 tons, but catch amount in the eastern Pacific Ocean has increased gradually since 2012 and fluctuated around 20,000 tons (**Appendix Figure 2**). Troll fishery mainly captures juvenile albacores in New Zealand's coastal waters and the central Pacific Ocean since the mid-1980s with the amount of total catch fluctuated around 2,000 tons (**Appendix Figure 3**). Driftnet vessels from Japan and Taiwan targeted albacore in the Tasman Sea and the central Pacific Ocean near the STCZ for a short period during the 1980s and early 1990s, but has since declined to zero following a United Nations moratorium on industrial-scale drift-netting in 1989 (Hoyle et al., 2012).

South Pacific albacore is managed by two Regional Fisheries Management Organizations, Western and Central Pacific Fisheries Commission (WCPFC) and Inter-American Tropical Tuna Commission (IATTC). The current management strategy provided by the WCPFC had forbidden any increase in fishing vessels south of 20 °S above 2005 levels (WCPFC CMM-2015-2). Although the recent stock assessment suggested that south Pacific albacore was not overfished, nor was overfishing occurred (Tremblay-Boyer et al., 2018), the decline in albacore biomass has raised concerns about the economic sustainability of the south Pacific albacore



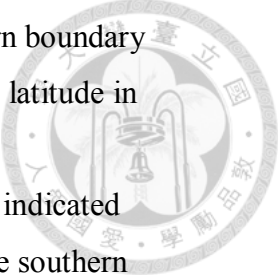
fisheries (Brouwer et al., 2019).



1.3 The impact of environmental variability and climate change

Understanding and predicting responses to global climate change are important issues for the scientific community to assist in designing effective fishery management to ensure the sustainability of the south Pacific albacore stock given that albacore fisheries provide significant economic, social, and cultural benefits to PICTs. Past studies have suggested that albacore's vertical distribution was constrained by thermal preference and their diet, they showed different vertical moving patterns in the tropical and temperate area (Williams et al., 2015). Langley and Hampton (2005) indicated that temperature is a key factor for albacore horizontal distribution and its movement tends to correspond to the seasonal oscillation of the location of the 23 - 28 °C isotherm of sea surface temperature. Brill (1994) suggested that dissolved oxygen (DO) is a good index of albacore habitat suitability that the reduced ambient oxygen levels would prolong the time required for albacore to recover from strenuous exercise. Salinity and chlorophyll-*a* concentrations were also suggested to be related to the albacore abundance and distribution through affecting the availability of their prey (Xu et al., 2013; Novianto and Susilo, 2016). Therefore, variability in these environmental variables at seasonal, inter-annual (El Niño Southern Oscillation, ENSO) and multi-decadal (Pacific Decadal Oscillation, PDO) time scales likely affect albacore tuna distributions. For example, studies suggested that the high catch rate of albacore has corresponded to the El Niño events (Zainuddin et al., 2004; Briand, 2011) and possible enhanced recruitment during the La Niña events (Lu et al., 1998; Lehodey, 2004).

Climate change has been suggested to have a significant impact on the marine ecosystems that influence species distribution (e.g., striped marlin, Su et al., 2013; pelagic squid, Alabia et al., 2016; anchovy, Silva et al., 2016; tunas, Erauskin-Extramiana et al., 2019). Longer-term trends in the oceanography of the Southern Hemisphere have also been detected (Ganachaud et al., 2011), which may have influenced the large scale

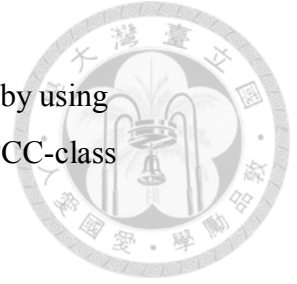


distribution of albacore. Lehodey et al. (2015) suggested that the northern boundary of south Pacific albacore distribution may shift southward by roughly 5° latitude in 2080 by using the Spatial Ecosystem and Population Dynamics Model (SEAPODYM). However, Senina et al. (2018) by using the same model indicated that the albacore distribution may remain stable in the western part of the southern Pacific Ocean in 2100, but may expand in the eastern Pacific Ocean without the hypothesized oxygen change. Erauskin-Extramiana et al. (2019) used a generalized additive model (GAM; Hastie, 1990) and indicated that the abundance is expected to decrease in temperate areas and the southern boundary of the distribution may shift southward in 2100. In general, the past studies have used a variety of approaches to model the future spatial and temporal variations of the south Pacific albacore distribution under climate change, but there were no consensus results. The uncertainty in future climatic conditions is one of the major sources of uncertainty in the species distribution projections under climate change (Beaumont et al., 2008). In this study, I aim to use an ensemble modelling approach to reduce the impact of uncertainty from various atmosphere-ocean general circulation models (AOGCMs) and anthropogenic emission scenarios of the Intergovernmental Panel on Climate Change (IPCC) fifth phase of the Coupled Model Intercomparison Project (CMIP5) on future albacore distribution under climate change (Araújo and New, 2007; Alabia et al., 2016).

1.4 Objectives

The south Pacific albacore stock generally refers to the albacore stock captured in the WCPFC convention area. In this study, the “south” Pacific albacore stock refers to the spatial coverage of available albacore data from both WCPFC and IATTC in the South Pacific Ocean. The objectives of this thesis are:

1. To quantify the relationship between albacore density and potential environmental variables by using a GAM approach.



2. To investigate the large-scale future distribution changes of albacore by using ensemble forecasts based on the environmental data projected by the IPCC-class AOGCMs under different degrees of ocean warming.

3. To evaluate the future change in albacore density within the exclusive economic zones (EEZs) of the countries and territories in the South Pacific Ocean and examine the implications of the current management measure (WCPFC CMM 2015-02).

The findings will be relevant for the south Pacific albacore stock management and will contribute to understanding the potential impacts of climate change on albacore fisheries.

Chapter 2 Materials and Methods

2.1 Fishery data

Catch and effort data grouped by quarter and $5^{\circ} \times 5^{\circ}$ grid cell for the longline fisheries for the south Pacific albacore was downloaded from the public domain dataset of the WCPFC (<https://www.wcpfc.int/public-domain>) and IATTC (<https://www.iattc.org/PublicDomainData/IATTC-Catch-by-species1.htm>). In addition, catch and effort data for the Taiwanese distant-water longline fishery for south Pacific albacore obtained from the Overseas Fisheries Development Council of Taiwan (<http://www.ofdc.org.tw/>) was used as a substitution of public domain dataset for the fleet as the best available data. Albacore nominal catch-per-unit-effort (CPUE, number/1000 hooks) calculated as a proxy for stock relative abundance for 1997 - 2016 was used for the analyses because only a small amount of data was available before 1997. The CPUE was calculated using the formula below:

$$CPUE_{y,q,i,f} = \frac{N_{y,q,i,f}}{E_{y,q,i,f}}$$

where N is the number of fish caught; E is the number of hooks (in thousands); y is year; q is quarter; i is the spatial location of the $5^{\circ} \times 5^{\circ}$ grid cell; f is the flag of longline fleet.

The longline fisheries dataset by flags included in this study were summarized in **Table 1**. The data grooming was applied to remove records outside of the temporal or spatial span of the analysis, or with improbable records. Records with missing logdates, 0 hooks, more albacore caught than the number of hooks, CPUE larger than 2 times the interquartile range (i.e., outliers) and vessels that were only present in the dataset for a very short period of time or small proportion ($< 1\%$) of catch, were all excluded from the dataset. In total, there are 17,393 records left, shown by flags in **Figure 1**, from 19,799 records (with 7% removal) after the initial cleaning.





2.2 Historical and future environmental data

Several environmental variables were evaluated for possible effects on the distribution of south Pacific albacore, based on Briand et al. (2011) and Novianto and Susilo (2016): sea surface temperature (SST, °C), sea surface salinity (SSS, PSU), mixed layer depth (MLD, m), dissolved oxygen concentration under 100m depth (DO100, mmol L⁻¹), chlorophyll-*a* concentration (CHL, kg L⁻¹). Monthly averaged satellite data [SST, SSS, MLD, DO100, and CHL] from 1997 to 2016 were used to characterize the environmental preferences of south Pacific albacore by using the GAM analysis (see 2.3.1 *Generalized additive models*). All satellite datasets were downloaded from the Copernicus -Marine environment monitoring service (<http://marine.copernicus.eu/>). All environmental datasets were rescaled to quarterly 5° × 5° spatial resolution based on the coarsest scale of longline fisheries data.

Projections of environmental variables for the reference period (1997 - 2016), current (2020), mid (2050), and late (2080) period of the 21st century were extracted from the IPCC CMIP5 with the Representative Concentration Pathways (RCP) 4.5 and 8.5 (van Vuuren et al., 2011) to generate historical and future potential south Pacific albacore habitat predictions. Environmental variables were downloaded from the Earth System Grid Federation (ESGF; <https://esgf-node.llnl.gov/projects/esgf-llnl/>). The RCP4.5 and 8.5 is characterized by the stabilization without overshoot pathway to 4.5 W m⁻² (650 ppm CO₂ eq) and by rising radiative forcing pathway leading to 8.5 W m⁻² (1370 ppm CO₂ eq), respectively, by 2100 (Thomson et al., 2011; Riahi et al., 2011). The list of the five AOGCMs used in this study was summarized in Table 2. The spatial resolution of AOGCMs-predicted environmental data varied from 0.3 - 1° × 1° to 1.5° × 1° (latitude by longitude). In this study, the predicted environmental data were interpolated to a 1° × 1° resolution for use in the forecasts of the spatial distribution of the south Pacific albacore. Some variables that showed high variation among the predictions

of AOGCMs, identified by the coefficient of variation (CV) larger than 100%, were not included in the further analysis (e.g., CHL).



2.3 Species distribution model

2.3.1 Generalized additive models

Species distribution models of the south Pacific albacore was constructed by modelling CPUEs in relation to environmental variables using generalized additive models (GAMs) (Hastie and Tibshirani, 1990; Wood, 2012, 2017). GAMs were selected because they enable the fit of nonlinear relationships with continuous and categorical variables by using smoothing functions. The raw CPUE data from the tuna longline fisheries includes many zeros. In this context, it was appropriate to fit the delta approach which models the probability of encounter of a fish population and the non-zero CPUE when fish are encountered (Pennington, 1983, 1996; Lo et al., 1992). Due to the low percentage of zero catches (< 10%) of the quarterly $5^\circ \times 5^\circ$ aggregated dataset that implying zero inflation was not an issue, I only fit the density model using the log-transformed CPUE of albacore, with a small constant (10% of the grand mean) added to avoid log-transformation problems (Howell and Kobayashi, 2006; Mugo et al., 2010). GAMs were built using the *gam* function of the “mgcv” package in R-language (Wood, 2012). First, I constructed a full model by including all explanatory variables, it can be written as:

$$\log(CPUE + 1) \sim \mu + Year + Quarter + Flag + s(SST) + s(SSS) + s(MLD) + s(DO100)$$

where μ is the intercept value; *Year*, *Quarter*, *Flag* are the fixed effect for year, quarter, and catchability of longline-fleet flag, respectively; and *s()* is a smoothing function for the explanatory covariates. To avoid overfitting, degrees of smoothness (“*k*” values) were set to less than or equal to 8 (Erauskin-Extramiana et al., 2019).

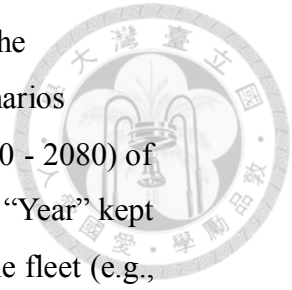
2.3.2 Variable selection and model validation

Five candidate models were selected by the dredge function of the “MuMIn” R-package (Barton, 2016). The function generates a subset of models with different combinations of variables of the full model, rank those models according to their Akaike information criterion (AIC) value, and percent of deviance explained (Bruge et al., 2016; Erauskin-Extramiana et al., 2019). Multicollinearity was tested by using the *ggpairs* function of the “GGally” R-package if any highly correlated environmental variables should be removed (Arrizabalaga et al., 2015). A pairwise correlation exceeds a threshold of 0.5 - 0.7 is defined as the presence of high collinearity (Dormann et al., 2013). The relative importance of predictor variables was evaluated by the percentage relative changes in the explained deviance and AIC of dropping each main effects factor from the full GAM (Kwon et al., 2018). Model performance of the top five candidate models was validated using *k*-fold cross-validation method. I used *k* = 5, data were randomly split into 5 subsets, using 80% of data to validate the remaining 20% (Erauskin-Extramiana et al., 2019; Georgian et al., 2019). For each model, the average R^2 value of training data and validation data were calculated as a measure for goodness-of-fit. I defined the model of average $R^2 > 0.6$ as a good prediction performance. A large difference between the training and testing R^2 would indicate overfitting (Villarino et al., 2015). The model with the lowest AIC and highest average R^2 value was selected as the best model (Brewer et al., 2016).

2.4 Historical and future albacore distribution projection

Historical environmental data projected by the AOGCMs were used as inputs in the GAM to estimate the albacore distribution in 1997-2016. The predicted density values were then compared with the observed CPUE from the longline fisheries in 1997- 2016 to evaluate the model performance for forecasting potential habitat. For estimating the future impacts of climate change on albacore distribution, the ensemble GAM projections (see 2.5 *Ensemble forecasting*) for the current (2020), mid (2050) and late (2080) periods

of the 21st century derived from the five AOGCMs were compared to the projections of recent five years of 2012 - 2016 under two emission scenarios (RCP4.5 and RCP8.5). In the future habitat distribution projection (2020 - 2080) of each AOGCM, model projections were performed with the fixed factor “Year” kept at the mid-year between 1997 and 2016. Flag factor was set to a longline fleet (e.g., TW) that simply represents a scaling parameter for the catchability. For some AOGCMs (IPSL and HadGEM) that certain environmental variables were unavailable (MLD and DO100), the quarterly average value derived from other GCMs was used as a substitute.



2.5 Ensemble forecasting

This study used ensemble analysis to deal with the uncertainty between climate models, it has been proved to outperform a single model in past studies (Diniz-Filho et al., 2009, Crimmins et al., 2013). In this study, I used two ensemble methods to measure the distribution of the south Pacific albacore. First, the consensus forecasting was made by calculating the median value of the GAM predictions based on the environmental data projected by five AOGCMs under the RCP4.5 and 8.5 scenarios, it was a measure of central tendency, therefore reduce inter-model variances propagated from the AOGCMs. Furthermore, the spatial distributions of density (number/1,000 hooks) anomalies of south Pacific albacore were calculated by subtracting the predictions from the median ensemble GAM projections by the current (2020), mid (2050), and late (2080) periods of the 21st century from the recent average of 2012-2016. The second ensemble approach used in this study was probabilistic forecasting. The set of grid cells that may be considered preferred habitats were defined as those for which predicted density from the GAM is in the top 15% (Su et al., 2013). Thus, the probability of preferred habitats at each $1^\circ \times 1^\circ$ cell was based on the percentage of five AOGCMs for which the predicted density at that location is considered preferred, called “agreement map” (Porfirio et al., 2014). Furthermore, spatial uncertainty of the predicted albacore distributions over five

AOGCMs (measured by CV) under the RCP scenarios were evaluated for the robustness of ensemble predictions.



2.6 *Expected changes in EEZs*

The potential density change (number/1000 hooks) averaged per grid cell for the south Pacific albacore under future climate change was estimated within the exclusive economic zones (EEZs) for the countries and territories in our study area. EEZ data (downloaded from <http://www.marineregions.org>) delimit the 200 nautical miles boundary from each coast (Flanders Marine Institute, 2018). This study only analyzed those countries or territories with more than 30% of the grid cells of fishery data inside the EEZ to ensure it was representative of relative abundance (Erauskin-Extramiana et al., 2019). For each RCP scenario, the density change was calculated by subtracting the predicted density of median ensemble during the main fishing season within each EEZ in 2020, 2050, and 2080 from that in the recent five years of 2012 - 2016.

Chapter 3 Results



3.1 Albacore distribution model

3.1.1 Variable selection & Model validation

The predicted environmental variables under the RCP4.5 and 8.5 scenarios were evaluated for the spatial uncertainty (measured by CV) in 2020, 2050, and 2080 among the five AOGCMs. The CHL showed highly spatial uncertainty in three future periods, mean CV ranged from 82% - 107%, among the CMIP5 climate models for both RCP scenarios compared to predictions of the SST (5.1% - 5.9%), MLD (43% - 45%), SSS (1.6% - 1.8%), and DO100 (7.2% - 7.8%) (**Appendix Figures 4 - 8**). For reducing the uncertainty of the future habitat distribution predictions, CHL was not included in the GAM model while the other variables (i.e., SST, SSS, MLD, and DO100) were kept for the analysis. Scatterplots between environmental variables suggested low collinearity that the absolute values of correlation coefficients are less than 0.5 (**Fig. 2**).

Results for each of the five candidate models (model, predictor variables, effective degrees of freedom, AIC, P -value, and deviance explained) selected by *dredge* function were shown in **Table 3**. In all the models, the smooth terms were highly significant ($P < 0.001$). Overall, the full GAM had the lowest AIC value and the highest deviance explained (62.1%). Variable rankings based on the percentage relative changes in the explained deviance and AIC for the three most influential explanatory variables were: 1) DO100; 2) Flag; and 3) SST (**Table 4**). Cross-validation testing suggested that the full GAM had the best performance, with the highest R^2 values for the training (0.62) and validation (0.61) datasets, compared to other candidate models. A negligible difference in the R^2 values indicated the absence of overfitting (**Table 5**). The residuals of the full GAM conform well to the assumption of lognormality based on the distribution of residuals (**Fig. 3a**) and quantile-quantile (QQ) plots (**Fig. 3b**). Therefore, the full GAM was selected as the best model for the future habitat distribution prediction.



3.1.2 GAM-derived habitat characteristics for albacore tuna

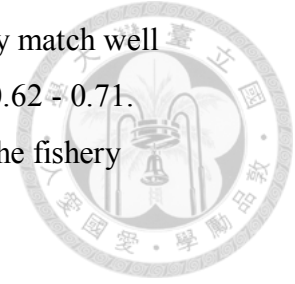
The response curves for environmental variables derived from the full GAM were interpreted in terms of habitat suitability of the south Pacific albacore (**Fig. 4**). The fitted smooth curves show the preferred SST range of 13 - 22 °C with a peak at around 15°C and SSS ranges of 34 - 35 PSU and > 36 PSU. Preferred MLD was between 20 m and 60 m and the DO100 between 0.2 and 0.25 mmol L⁻¹. Approximate confidence interval envelopes were also plotted for each function. Lower accuracy was observed in the estimations for lower values of SST (< 15 °C), SSS (< 34 PSU), DO100 (< 0.1 mmol L⁻¹) and higher values of MLD (>100 m) and DO100 (> 0.25 mmol L⁻¹) because of fewer data. The estimates of the year, quarter, and flag factors from the GAM were shown in **Figure 5**. The year factor showed a significant decline during 1997 - 2003 and increase during 2004-2010. There is a significant seasonal variation in the quarter factor with the higher estimates in quarters 2 and 3. The flag factor showed higher estimates for CK, NC, US, and WS, but lower estimates for FM, AU, JP, KR, and NZ.

3.2 Albacore distribution in the historical fishing period

South Pacific albacore was widely distributed between 0° - 50 °S with higher density in the temperate areas (30 - 40 °S) of central Pacific Ocean, the Tasman Sea between Australia and New Zealand, and 80° - 100 °W and 20° - 30 °S of the eastern Pacific Ocean based the ensemble GAM projections during 1997 - 2016 (**Appendix Figures 9 - 10**). Annual aggregated CPUE values superimposed on the projected distributions with the Pearson correlation coefficients (*r*) ranged from 0.41 – 0.68 indicated that the ensemble approach could generally yield reliable predictions overtime except for 2002.

Quarterly average distribution of albacore during 1997-2016 was shown in **Figure 6**. Model prediction has mimicked a clear north-south seasonal variation of albacore

distribution. The predicted spatial distributions in quarters 2-4 generally match well with the CPUE of longline vessels, in which the r values ranged from 0.62 - 0.71. However, the prediction fitted relatively poorly in the first quarter for the fishery data located north of 35 °S ($r = 0.6$).



3.3 Future projections

3.3.1 Future environment

The spatial distributions of the medians of the environmental variables derived from the five AOGCMs for the current (2020), mid (2050), and late (2080) periods of the 21st century by each RCP scenario were shown in the **appendix figures 11 - 14**. A slight increase of projected SST was observed in 2050 and 2080 under the RCP4.5 that the pronounced changes occurred in the temperate latitudes south of 30 °S. Under the RCP8.5, the SST have increased largely during 2020 - 2080 in the entire studied region and the MLD decreased in the eastern waters off New Zealand in 2080. Declines of DO100 were observed in 2050 and 2080 within the area north of 15 °S for both RCP scenarios. However, other environmental variables showed minimal changes over the projected future periods either in the RCP4.5 or 8.5 scenarios.

Annual time-series of the areal-averaged of the environmental variables from 2020 - 2080 projected by the five AOGCMs were shown in **Figure 7**. The predicted levels of environmental changes across the five AOGCMs exhibited differences in the magnitude, for example, the lowest SST predictions by the IPSL and the highest by the HadGEM. Under the RCP4.5, the median value was expected to increase from 20.8 to 21.1°C for SST, decrease from 81.3 to 73.9 m for MLD, and decrease from 0.22 to 0.218 mmol L⁻¹ for DO100, respectively, during 2020-2080, while no trend was found in the SSS. Under the RCP8.5, the more pronounced changes in SST with 2°C warming and in MLD with 12 m shallowed were observed during

2020 - 2080.

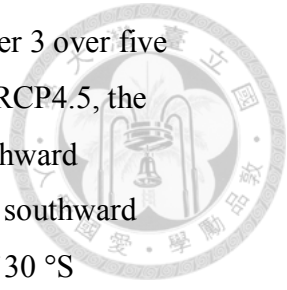


3.3.2 Projection of future albacore distribution

The median-ensemble albacore distribution prediction in quarter 3 of 2020 across five AOGCMs was illustrated in **Figure 8** because quarter 3 contains the highest fisheries harvest (36%). The albacore distribution predictions varied among various models that the preferred habitat (defined as CPUE > 25 number/1000 hooks) was predicted to expand widely in the eastern Pacific (25 - 40 °S and 80 - 130 °W) for the MPI climate model (**Fig. 8d**), but mainly occurred in the western Pacific for the CanESM and HadGEM climate models (**Fig. 8b and e**). However, the ensemble of prediction showed a robust result in opposition to the inter-model uncertainty (**Fig. 8f**).

The future ensemble projections of albacore distributions in quarter 3 derived from the five AOGCMs for the current (2020), mid (2050), and late (2080) periods of the 21st century by each RCP scenario were shown in **Figure 9**. The northern boundary of albacore preferred habitat in the western Pacific was projected to shift southward from 20 °S in 2020 to 22 °S in 2050 and 25 °S in 2080 for the RCP4.5. A similar pattern of southward shifting was observed for the RCP8.5, with a wider spatial extent compared to the RCP4.5. More specifically, the northern boundary has shown a similar degree of shifting as RCP4.5, while the southern boundary in the Tasman Sea has shifted from 40 °S in 2020 to 43 °S in 2050 and 45 °S in 2080.

Figure 10 shows the spatial distributions of density anomalies in quarter 3 by 2020, 2050, and 2080 under two RCP scenarios. The potential albacore habitats increased in the latitudes of 30 - 40 °S but decreased in 20 - 30 °S of the western Pacific in 2020, 2050, and 2080 for the RCP4.5, that the pattern of the gains and losses of potential habitat has become more apparent overtime. A similar pattern was observed for the RCP8.5, however, the potential albacore habitats increased in the higher latitudes south of 40 °S in 2080 in the western Pacific, especially in the Tasman Sea, and in the eastern Pacific (east of 110 °W) during 2020 - 2080 compared to RCP4.5.



Ensemble agreement maps for future albacore distribution in quarter 3 over five AOGCMs under two RCP scenarios were shown in **Figure 11**. For the RCP4.5, the core habitats in western Pacific (red areas in **Fig. 11a**) have shifted southward slightly during 2020 - 2080. The habitat ranges (blue areas) also shifted southward with an increase of 15% by 2050 and 16 % by 2080 in the area south of 30 °S relative to 2020, respectively. A similar southward displacement was also observed under the RCP8.5 (**Fig. 11b**), the latitudinal boundaries of core habitats showed an obvious southward shift in the Tasman Sea from 25 - 32 °S in 2020 to 27 - 36 °S in 2050 and to 32 - 39 °S in 2080, respectively, and the habitat ranges in the area south of 30 °S increased 15% in 2050 and 21% in 2080.

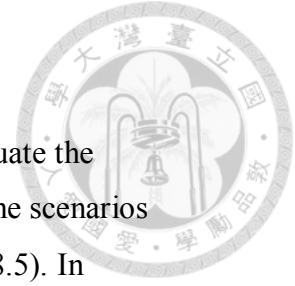
Spatial uncertainty (measured by CV) in quarter 3 estimated from the five AOGCMs by each RCP scenario was shown in **Figure 12**. A consistent pattern of high CVs (> 0.5) in the areas around Solomon Islands (5 - 15 °S and 150 - 180 °E) and in the areas south of 40 °S was found in 2020, 2050, and 2080 for the RCP4.5. While both RCP scenarios generally exhibited a similar spatial pattern in uncertainty overtime, the RCP8.5 showed high CVs in the central Pacific north of 20 °S in 2080. In general, the spatial uncertainty remained low ($CV < 0.5$) in the habitat ranges indicated the robust predictions of albacore distribution under climate change.

3.3.3 *Albacore density changes in EEZs*

The results of the projected changes in albacore density during the main fishing season within the EEZs in 2020, 2050, and 2080 relative to 2012 - 2016 under the RCP4.5 and 8.5 scenarios were shown in **Figure 13**. Under the RCP4.5, albacore density is projected to decrease in most EEZs overtime (by about 25% in 2080), but was projected to slightly increase in 2020 and then decreased after 2050 for the EEZs of Kiribati (KI), Tuvalu (TV) and Tokelau (TK) (**Fig. 13a**). The EEZ of New Caledonia (NC) has the greatest projected depletion in density by 2080 (43%). The density is projected to increase by 13% and 21% by 2080 in the EEZs of New

Zealand (NZ) and Norfolk Island (NK), respectively. Similar patterns of density decline in most EEZs overtime were found for the RCP8.5 (**Fig. 13b**). A more significant negative and positive impact on the change of albacore density in 2080 was found for the EEZs of NC and both NZ and NK, respectively. The decline of density in 2080 for the EEZ of Australia (AUS) was slightly improved in RCP8.5 (-2%) compared to RCP4.5 (-11%).

Chapter 4 Discussion



In this study, I developed an ensemble forecast framework to evaluate the projected future potential distribution of south Pacific albacore under the scenarios of intermediate and high degrees of ocean warming (RCP4.5 and RCP8.5). In general, the spatial uncertainty remained low ($CV < 0.5$) in the predicted habitat ranges indicated robust predictions by using the median ensemble forecasts. The northern boundary of albacore preferred habitat is expected to shift southward by about 5° latitude and the density is expected to gradually increase south of 30°S from 2020 to 2080 for both RCP scenarios, especially with a higher degree of change for the RCP8.5. This study highlights that investigating the future spatio-temporal patterns of the potential albacore habitats could lend significant implications on the availability of tuna resources to the fishery and subsequent evaluation of tuna fishery management options under climate change.

The results of this study may be considered as reliable predictions of the south Pacific albacore because the data used has contained a substantial amount ($> 90\%$) of the albacore catch and included all fleets covered a wide geographical range of the convention areas of the WCPFC and IATTC. Erauskin-Extramiana et al. (2019) only used the Japanese longline fishery data, constrained in the areas of 20°S northward and the waters off the eastern coast of Australia, which may not be informative to characterize the habitat preferences of albacore. Although the raw CPUE variability among various flags have been addressed in the GAM, the results with catchability adjustment can be biased due to the time-variant changes in fishing processes (e.g., gear, fishing power, and fishing behavior). For example, the targeting tactic by Taiwanese distant water longline fishery has changed over time from only targeting albacore to both tropical tuna (mainly bigeye and yellowfin) and albacore (Chang et al., 2011). We recommend that the future albacore distribution model should further consider the fisheries targeting behaviors to adjust the potential confounding effects on the estimation of relative abundance for the fishery-

dependent CPUE data (Winker et al., 2013).

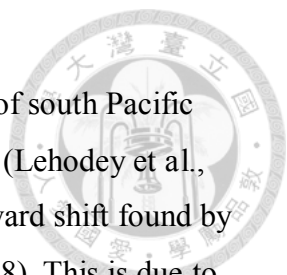
The south Pacific longline fisheries tend to exploit the larger size of albacore (> 80 cm FL) (Scott and Mckechnie, 2015) while the juvenile albacore is mainly targeted by the troll fishery near the coastal area of New Zealand. The projected results of this study may be considered as a proxy for the adult population. This highlights that using data from other types of fishing gear (i.e., troll fishery) may provide additional information to better understand the ontogenetic habitat preferences of the south Pacific albacore in future analysis.

The GAM used in this study was shown to robustly fit the data (deviance explained = 62%) because the residuals (in log-space) for the lognormal error distribution appear normal. Cross-validation testing also suggested that the GAM performed well without overfitting. However, quarter 1, not represents the main fishing season of albacore, had a relatively poor model performance compared to other quarters. The albacore may prefer a variety of habitat conditions in quarter 1 because some spawning adults in the second phase of spawning season are present in the tropical habitat of warmer temperature, but a large portion returns to their favorable feeding zones driven by the local cues in feeding habitat (Senina et al., 2019). A further extension of the GAM would be to estimate a seasonally variant habitat effect within the model, potentially improving the uncertainty of seasonal predictions. However, this was outside the scope of this study.

This study used a long-time series dataset (20 years of longline catch and effort data) with a wide range of observations for quantifying the relationships between the environmental variables and albacore catch rate, which improves the reliability of albacore response curve. Although all the environmental variables included in this study showed statistically significant impacts on albacore's catch rate, the spatial distribution of albacore may be influenced by other factors in addition to the environmental variables used in the GAM. A range of observed or satellite-based oceanographic and biological variables has also been used to describe albacore-environment associations, including

meridional and zonal geostrophic currents, sea surface height, thermal fronts, eddies, meso-zooplankton biomass over 0-100 m (Zainuddin et al., 2006; Lan et al., 2012; Xu et al., 2013; Arrizabalaga et al., 2015). However, one of the major issues to explore a broad range of oceanographic and biological variables for evaluating the future distribution shift is the availability of those variables from the future climate models. Furthermore, with a highly uncertain future environment, the predictions from AOGCMs could change in large amounts among each other compared to the historical predictions (e.g., CHL in this study). The above issues prevented further improvement for this study.

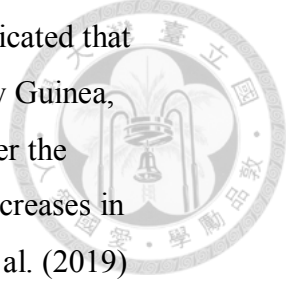
This study indicated that DO100 is the predominant environmental predictor of the distribution of south Pacific albacore because it contributed a substantial amount of explanatory power (22%) to the GAM. The albacore habitat was expected to decrease in the north of 15°S under the influence of a decrease in DO100 projected by the AOGCMs. The strong association between DO concentration and albacore distribution was confirmed by Lehodey et al. (2015) and Senina et al. (2018) through the sensitivity analysis in SEAPODYM that the future distribution and abundance of albacore tuna is likely to significantly decrease and remain stable in the South Pacific Ocean with and without a projected decrease in DO, respectively. The empirical study also supports the sensitivity of DO that albacore is not tolerant to low DO concentration compared to other tunas (Brill, 1994). On the other hand, studies indicated that albacore is highly sensitive to the temperature changes in both their spawning and feeding environments (Williams et al., 2015; Reglero et al., 2017), which is in agreement with the GAM analysis of this study that SST is considered as the second most important environmental factor (6%). Furthermore, the pronounced spatial changes in potential future albacore habitats could be also explained by the substantial changes in projected SST under ocean warming scenarios. This emphasizes that accuracy and precision in ensemble forecasts of albacore tuna distribution are fundamentally linked to the performance of the AOGCMs in being able to realistically describe future changes in DO and SST.



The southward distribution shift and changes in habitat suitability of south Pacific albacore identified in this study are consistent with the previous studies (Lehodey et al., 2015; Erauskin-Extramiana et al., 2019). However, the expected southward shift found by the above studies did not agree well with the study by Senina et al. (2018). This is due to the temperature spawning function implemented in SEAPODYM by Senina et al. (2018) tends to estimate a warmer favorable spawning habitat, resulted in future projected spawning ground similar to the present day. This indicated the importance of understanding the biological mechanism associated with shifts in albacore spawning ground under ocean warming. In addition, the distribution of albacore could be strongly influenced by the changes in growth, reproduction, and survival rate, and therefore the relevant mechanisms should be investigated in further analysis.

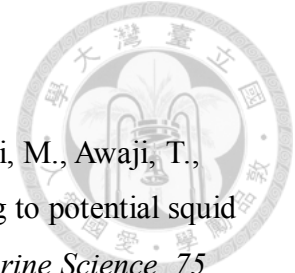
The uncertainty among the projections from the five AOGCMs and the two ocean warming scenarios that represent the plausible atmospheric forcings and emission pathways was taken into account through the ensemble analysis in this study. In addition to the uncertainty of climate projections, it would be desirable to explore other species distribution modelling approaches (e.g., Random forest, Maximum entropy, Boosted regression tree models) to reduce the risk that structural inadequacies, inappropriate parameter specifications, or bias in each approach may unduly influence the final outputs (Robert et al., 2016; Georgian et al., 2019). Although ensemble forecasting could emphasize the ‘signal’ that one is interested in emerges from the ‘noise’ associated with individual model errors and uncertainties, the overall ensemble accuracy remains dependent on individual predictions (Araujo and New, 2007). Therefore, better individual forecasts will provide better combined forecast. Despite these issues, the ensemble forecasting approach could substantially reduce the likelihood of making false management decisions based on predictions that are far from the truth.

In this study, albacore abundance is projected to decrease in most EEZs by 2080 with the greatest depletion for New Caledonia, but is projected to increase for New

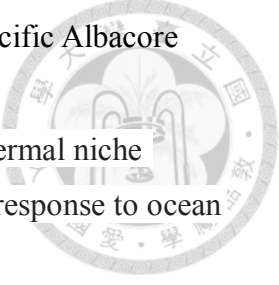



Zealand and Norfolk Island. The projections by Senina et al. (2018) indicated that the largest biomass increases occurred in the EEZs of Palau, Papua New Guinea, Federated States of Micronesia and Nauru at the end of the century under the simulation scenario with projected changes in DO concentration, but decreases in the EEZs of Fiji, New Caledonia, and Vanuatu. Erauskin-Extramiana et al. (2019) suggested that the south Pacific albacore abundance would decrease in Kiribati, Tuvalu, Tokelau, Cook Islands, and Australia, but an increase in New Zealand. The result of this study generally supports the published evidence of the expected changes of albacore abundance in EEZs of PICTs except for the Palau, Federated States of Micronesia, and Nauru. The reason why those EEZs was not identified is because the present study only analyzed the countries or territories with more than 30% of the grid cells of fishery data inside the EEZs. Although the present study showed a decrease of abundance for Australia compared to the identified increase by Erauskin-Extramiana et al. (2019), Australia was found to have the smallest decrease of abundance among all countries and territories that located in the study area under the RCP8.5. Currently, the conservation management measure (CMM) of south Pacific albacore by the WCPFC has forbidden any increase in fishing vessels south of 20 °S above 2005 levels (CMM-2015-2). Under the current fishing effort constraint by the CMM, the future harvest catch of south Pacific albacore is expected to decrease because the potential albacore habitats are likely to increase in the latitudes of 30 - 40 °S but decreased in 20 - 30 °S of the western Pacific. This suggests that the effectiveness of current CMM to achieve the fishery management goals could be impacted by the future potential distribution shifting. I assert not only the need but also the feasibility of incorporating approaches to address such shifts directly in the analysis of stocks and the management (e.g., management strategies evaluation, Punt et al., 2016) based thereon, so that the stock can be managed in a proactive and precautionary manner.

References

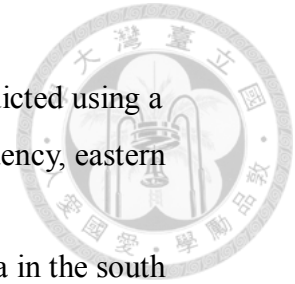



- Alabia, I. D., Saitoh, S. I., Igarashi, H., Ishikawa, Y., Usui, N., Kamachi, M., Awaji, T., and Seito, M. (2016). Future projected impacts of ocean warming to potential squid habitat in western and central North Pacific. *ICES Journal of Marine Science*, 75, 1343–1356.
- Arrizabalaga, H., Costas, E., Juste, J., González-Garcés, A., Nieto, B., and López-Rodas, V. (2004). Population structure of albacore *Thunnus alalunga* inferred from blood groups and tag-recapture analyses. *Marine Ecology Progress Series* 282, 245–252.
- Arrizabalaga, H., Dufour, F., Kell, L., Merino, G., Ibaibarriaga, L., Chust, G., Irigoien, X., Santiago, J., Murua, H., Fraile, I., Chifflet, M., Goikoetxea, N., Sagarminaga, Y., Aumont, O., Bopp, L., Herrera, M., Fromentin, M., and Bonhomeau, A. (2015). Global habitat preferences of commercially valuable tuna. *Deep Sea Research Part II: Topical Studies in Oceanography*, 113, 102–112.
- Araújo, M. B., and New, M. (2007). Ensemble forecasting of species distributions. *Trends in ecology & evolution*, 22(1), 42-47.
- Barton, K. (2016). Package “MuMIn”: Multi-Model Inference. R package, Version 1.15.6. URL: <https://cran.r-project.org/web/packages/MuMIn/index.html> [accessed 2016-10-22].
- Brewer, M. J., Butler, A., and Cooksley, S. L. (2016). The relative performance of AIC, AICC and BIC in the presence of unobserved heterogeneity. *Methods in Ecology and Evolution*, 7(6), 679-692.
- Brill, R. W. (1994). A review of temperature and oxygen tolerance studies of tunas pertinent to fisheries oceanography, movement models and stock assessments. *Fisheries Oceanography*, 3(3), 204-216.
- Briand, K., Molony, B., and Lehodey, P. (2011). A study on the variability of albacore (*Thunnus alalunga*) longline catch rates in the southwest Pacific Ocean. *Fisheries Oceanography*, 20(6), 517-529.
- Brouwer, S., Pilling, G., and Williams, P. (2018). Trends in the South Pacific Albacore Longline and Troll Fisheries. WCPFC-SC14-2018/ SA-IP-08 Rev. 2.

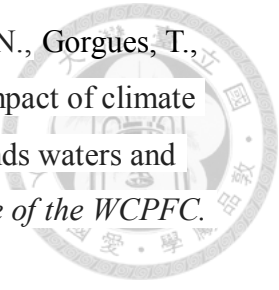
- 
- Brouwer, S., Pilling, G., and Williams, P. (2019). Trends in the South Pacific Albacore Longline and Troll Fisheries. WCPFC-SC15-2019/ SA-WP-08.
- Bruge, A., Alvarez, P., Fontán, A., Cotano, U., and Chust, G. (2016). Thermal niche tracking and future distribution of Atlantic mackerel spawning in response to ocean warming. *Frontiers in Marine Science*, 3, 86.
- Chang, S. K., Hoyle, S., and Liu, H. I. (2011). Catch rate standardization for yellowfin tuna (*Thunnus albacares*) in Taiwan's distant-water longline fishery in the Western and Central Pacific Ocean, with consideration of target change. *Fisheries Research*, 107(1-3), 210-220.
- Childers, J., Snyder, S., and Kohin, S. (2011). Migration and behavior of juvenile North Pacific albacore (*Thunnus alalunga*). *Fisheries Oceanography*, 20(3), 157-173.
- Collette, B. B., and Nauen, C. E. (1983). Scombrids of the world: an annotated and illustrated catalogue of tunas, mackerels, bonitos, and related species known to date. v. 2.
- Crimmins, S. M., Dobrowski, S. Z. and Mynsberge, A. R. (2013). Evaluating ensemble forecasts of plant species distributions under climate change. *Ecological Modelling*, 266, 126–130.
- Diniz-Filho, J. A. F., Mauricio Bini, L., Fernando Rangel, T., Loyola, R. D., Hof, C., Nogués-Bravo, D., and Araújo, M. B. (2009). Partitioning and mapping uncertainties in ensembles of forecasts of species turnover under climate change. *Ecography*, 32(6), 897-906.
- Dormann, C.F., Elith, J., Bacher, S., Buchmann, C., Carl, G., Carré, G., Marquéz, J.R.G., Gruber, B., Lafourcade, B., Leitão, P.J., Münkemüller, T., McClean, C., Osborne, P.E., Reineking, B., Schröder, B., Skidmore, A.K., Zurell, D., and Lautenbach, S. (2013). Collinearity: a review of methods to deal with it and a simulation study evaluating their performance. *Ecography* 36:27–46
- Erauskin-Extramiana, M., Arrizabalaga, H., Hobday, A. J., Cabré, A., Ibaibarriaga, L., Arregui, I., Murua, H., and Chust, G. (2019). Large-scale distribution of tuna species in a warming ocean. *Global Change Biology*. 25, 2043–2060.
- Farley, J. H., Hoyle, S. D., Eveson, J. P., Williams, A. J., Davies, C. R., and Nicol, S. J.

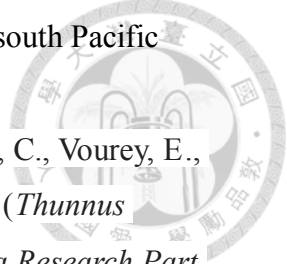
- 
- (2014). Maturity ogives for South Pacific albacore tuna (*Thunnus alalunga*) that account for spatial and seasonal variation in the distributions of mature and immature fish. *PloS one*, 9(1), e83017.
- FAO (2018). The state of World fisheries and aquaculture 2018. Food And Agriculture Organization of the United Nations. Fisheries and Aquaculture Department, Rome, Italy.
- Georgian, S. E., Anderson, O. F., and Rowden, A. A. (2019). Ensemble habitat suitability modeling of vulnerable marine ecosystem indicator taxa to inform deep-sea fisheries management in the South Pacific Ocean. *Fisheries Research*, 211, 256-274.
- Glaser, S. M., Waechter, K. E., and Bransome, N. C. (2015). Through the stomach of a predator: regional patterns of forage in the diet of albacore tuna in the California Current System and metrics needed for ecosystem-based management. *Journal of Marine Systems*, 146, 38-49.
- Gloria, M. B. A., Daeschel, M. A., Craven, C., and Hilderbrand Jr, K. S. (1999). Histamine and other biogenic amines in albacore tuna. *Journal of Aquatic Food Product Technology*, 8(4), 55-69.
- Ganachaud, A.S., Sen Gupta, A., Orr, J.C., Wijffels, S.E., Ridgway, K.R., Hemer, M.A., Maes, C., Steinberg, C.R., Tribollet, A.D., Qiu, B., and Kruger, J.C. (2011). Observed and expected changes to the tropical Pacific Ocean. In: Bell J, Johnson JE, Hobday AJ (eds) Vulnerability of tropical pacific fisheries and aquaculture to climate change. Secretariat of the Pacific Community, Noumea, pp 115–202.
- Hastie, T. J., and Tibshirani, R. J. (1990). *Generalized additive models* (Vol. 43). CRC press.
- Howell, E. A., and Kobayashi, D. R. (2006). El Nino effects in the Palmyra Atoll region: oceanographic changes and bigeye tuna (*Thunnus obesus*) catch rate variability. *Fisheries Oceanography*, 15(6), 477-489.
- Hoyle, S., Hampton, J., and Davies, N. (2012). Stock assessment of albacore tuna in the South Pacific Ocean. In *7th Meeting of the Scientific Committee of the Western and Central Pacific Fisheries Commission*. Pohnpei, Federated States of Micronesia

- (pp. 1-90).
- Kwon, Y., Larsen, C. P., and Lee, M. (2018). Tree species richness predicted using a spatial environmental model including forest area and frost frequency, eastern USA. *PloS one*, 13(9), e0203881.
- Langley, A., and Hampton, J. (2005). Stock assessment of albacore tuna in the south Pacific Ocean. Working Paper SA-WP-3, 1st Scientific Committee meeting of the Western and Central Pacific Fisheries Commission, Noumea, New Caledonia. (pp. 1-64)
- Lan, K. W., Kawamura, H., Lee, M. A., Lu, H. J., Shimada, T., Hosoda, K., and Sakaida, F. (2012). Relationship between albacore (*Thunnus alalunga*) fishing grounds in the Indian Ocean and the thermal environment revealed by cloud-free microwave sea surface temperature. *Fisheries research*, 113(1), 1-7.
- Lehodey, P. (2004). Climate and fisheries: an insight from the central Pacific Ocean. *Marine Ecosystems and Climate Variation: The North Atlantic. A Comparative Perspective*, 137.
- Lehodey, P., Senina, I., Nicol, S., and Hampton, J. (2015). Modelling the impact of climate change on South Pacific albacore tuna. *Deep Sea Research Part II: Topical Studies in Oceanography*, 113, 246-259.
- Leroy, B., and Lehodey, P. (2004). Note on the growth of the South Pacific albacore. In Presented at the 17th Meeting of the Standing Committee on Tuna and Billfish, 8–18 August, 2004.
- Lo, N. C. H., Jacobson, L. D., and Squire, J. L. (1992). Indices of relative abundance from fish spotter data based on delta-lognormal models. *Canadian Journal of Fisheries and Aquatic Sciences*, 49(12), 2515-2526.
- Lu, H. J., Lee, K. T., and Liao, C. H. (1998). On the relationship between El Nino/Southern oscillation and South Pacific albacore. *Fisheries Research*, 39(1), 1-7.
- Mugo, R., Saitoh, S. I., Nihira, A., and Kuroyama, T. (2010). Habitat characteristics of skipjack tuna (*Katsuwonus pelamis*) in the western North Pacific: a remote sensing perspective. *Fisheries Oceanography*, 19(5), 382-396.



- 
- Novianto, D., and Susilo, E. (2016). Role of sub surface temperature, salinity and chlorophyll to albacore tuna abundance in Indian Ocean. *Indonesian Fisheries Research Journal*, 22(1), 17-26.
- Pennington, M. (1983). Efficient estimators of abundance, for fish and plankton surveys. *Biometrics*, 281-286.
- Pennington, B. F., and Ozonoff, S. (1996). Executive functions and developmental psychopathology. *Journal of child psychology and psychiatry*, 37(1), 51-87.
- Porfirio, L. L., Harris, R. M., Lefroy, E. C., Hugh, S., Gould, S. F., Lee, G., Bindoff, N. L., and Mackey, B. (2014). Improving the use of species distribution models in conservation planning and management under climate change. *PLoS One*, 9(11), e113749.
- Punt, A. E., Butterworth, D. S., de Moor, C. L., De Oliveira, J. A., and Haddon, M. (2016). Management strategy evaluation: best practices. *Fish and Fisheries*, 17(2), 303-334.
- Ramón, D., and Bailey, K. (1996). Spawning seasonality of albacore, *Thunnus alalunga*, in the South Pacific Ocean. *Fishery Bulletin*, 94(4), 724-733.
- Reglero, P., Santos, M., Balbín, R., Lai'z-Carrión, R., AlvarezBerastegui, D., Ciannelli, L., Jimenez, E., Alemany, F. (2017). Environmental and biological characteristics of Atlantic bluefin tuna and albacore spawning habitats based on their egg distributions. *Deep Sea Research Part II: Topical Studies in Oceanography*, 140: 105–116.
- Riahi, K., Rao, S., Krey, V., Cho, C., Chirkov, V., Fischer, G., Kindermann, G., Nakicenovic, N. and Rafaj, P. (2011). RCP 8.5 - A scenario of comparatively high greenhouse gas emissions. *Climatic Change*, 109(1-2), 33.
- Robert, K., Jones, D. O., Roberts, J. M., and Huvenne, V. A. (2016). Improving predictive mapping of deep-water habitats: Considering multiple model outputs and ensemble techniques. *Deep Sea Research Part I: Oceanographic Research Papers*, 113, 80-89.
- Scott, R., and McKeachie, S. (2015). Analysis of Longline Length Frequency Compositions for South Pacific Albacore. WCPFC-SC11-2015/SA-IP-06.

- 
- Senina, I., Lehodey, P., Calmettes, B., Dessert, M., Hampton, J., Smith, N., Gorgues, T., Aumont, O., Lengaigne, M., Nicol, S., and Gehlen M. (2018). Impact of climate change on tropical Pacific tuna and their fisheries in Pacific Islands waters and high seas areas. *14th Regular Session of the Scientific Committee of the WCPFC. Busan, Republic of Korea.*
- Senina, I. N., Lehodey, P., Hampton, J., and Sibert, J. (2019). Quantitative modelling of the spatial dynamics of South Pacific and Atlantic albacore tuna populations. *Deep Sea Research Part II: Topical Studies in Oceanography*, 104667.
- Silva, C., Andrade, I., Yáñez, E., Hormazabal, S., Barbieri, M. Á., Aranís, A., and Böhm, G. (2016). Predicting habitat suitability and geographic distribution of anchovy (*Engraulis ringens*) due to climate change in the coastal areas off Chile. *Progress in Oceanography*, 146, 159-174.
- Su, N. J., Sun, C. L., Punt, A. E., Yeh, S. Z., DiNardo, G., and Chang, Y. J. (2013). An ensemble analysis to predict future habitats of striped marlin (*Kajikia audax*) in the North Pacific Ocean. *ICES Journal of Marine Science*, 70(5), 1013-1022.
- Thomson, A. M., Calvin, K. V., Smith, S. J., Kyle, G. P., Volke, A., Patel, P., Delgado-Arias, S., Bind-Lamberty, B., Wise, M.A., Clarke, L.E & Edmonds, J. A. (2011). RCP4. 5: a pathway for stabilization of radiative forcing by 2100. *Climatic change*, 109(1-2), 77.
- Tremblay-Boyer, L., Hampton, J., McKechnie, S., and Pilling, G. (2018). Stock assessment of South Pacific albacore tuna. *14th Regular Session of the Scientific Committee of the WCPFC. Busan, Republic of Korea.*
- van Vuuren, D. P., Edmonds, J., Kainuma, M., Riahi, K., Thomson, A., Hibbard, K., Hurtt, G. C., Kram, T., Krey, V., Lamarque, J., Masui, T., Meinshausen, M., Nakicenovic, N., Smith, S.J., and Rose, S. (2011). The representative concentration pathways: an overview. *Climatic change*, 109(1-2), 5.
- Villarino, E., Chust, G., Licandro, P., Butenschön, M., Ibaibarriaga, L., Larrañaga, A., and Irigoien, X. (2015). Modelling the future biogeography of North Atlantic zooplankton communities in response to climate change. *Marine Ecology Progress Series*, 531, 121-142.

- 
- WCPFC CMM-2015-02. Conservation and Management Measures for south Pacific albacore. 5-9. Dec. 2015, Kuta, Bali, Indonesia.
- Williams, A.J., Allain, V., Nicol, S.J., Evans, K.J., Hoyle, S.D., Dupoux, C., Vourey, E., and Dubosc, J. (2015). Vertical behavior and diet of albacore tuna (*Thunnus alalunga*) vary with latitude in the South Pacific Ocean. *Deep Sea Research Part II: Topical Studies in Oceanography*, 113, 154-169.
- Winker, H., Kerwath, S. E., and Attwood, C. G. (2013). Comparison of two approaches to standardize catch-per-unit-effort for targeting behaviour in a multispecies hand-line fishery. *Fisheries Research*, 139, 118-131.
- Wood, S. (2012). mgcv: Mixed GAM Computation Vehicle with GCV/AIC/REML smoothness estimation. R package version 1.7-17
- Wood, S. (2017). *Generalized Additive Models: an introduction with R* (2nd edition), CRC press.
- Xu, Y., Teo, S. L., and Holmes, J. (2013). Environmental Influences on Albacore Tuna (*Thunnus alalunga*) Distribution in the Coastal and Open Oceans of the Northeast Pacific: Preliminary Results from Boosted Regression Trees Models. International Scientific Committee Albacore Working Group. ISC/13/ALBWG-01/01.
- Zainuddin, M., Saitoh, S. I., and Saitoh, K. (2004). Detection of potential fishing ground for albacore tuna using synoptic measurements of ocean color and thermal remote sensing in the northwestern North Pacific. *Geophysical Research Letters*, 31(20).
- Zainuddin, M., Kiyofuji, H., Saitoh, K., and Saitoh, S. I. (2006). Using multi-sensor satellite remote sensing and catch data to detect ocean hot spots for albacore (*Thunnus alalunga*) in the northwestern North Pacific. *Deep Sea Research Part II: Topical Studies in Oceanography*, 53(3-4), 419-431.

Tables

Table 1. Summary of the longline fleets by flags used in the GAM analysis.

Flag code	Country/territory
AU	Australia
BZ	Belize
CN	China
CK	Cook Islands
FM	Federated States of Micronesia
FJ	Fiji
JP	Japan
KI	Kiribati
KR	Korea
NC	New Caledonia
NZ	New Zealand
PG	Papua New Guinea
PF	French Polynesia
SB	Solomon Islands
TO	Tonga
TV	Tuvalu
TW	Taiwan
US	United States of America
VU	Vanuatu
WS	Samoa



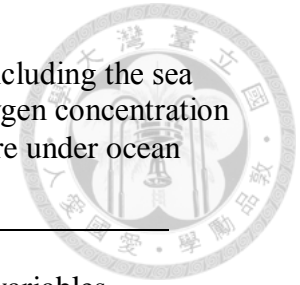


Table 2. List of IPCC atmosphere-ocean general circulation models where the future environmental variables, including the sea surface temperature (SST, °C), sea surface salinity (SSS, PSU), mixed layer depth (MLD, m), and dissolved oxygen concentration under 100m depth (DO100, mmol L⁻¹), were obtained to generate potential habitat maps of south Pacific albacore under ocean warming scenarios (RCP4.5 and RCP8.5).

Institute	Code	Source resolution	Included environmental variables
Canadian Earth System Model	CanESM	1.5° × 1°	SST, SSS, MLD, CHL*
Geophysical Fluid Dynamics Laboratory	GFDL	0.3 - 1° × 1°	SST, SSS, MLD, CHL*
Hadley Centre Global Environmental Model	HadGEM	0.3 - 1° × 1°	SST, SSS, CHL*
Institute Pierre Simon Laplace	IPSL	1° × 1°	SST, SSS, MLD, CHL*, DO100
Max Planck Institute for Meteorology	MPI	1° × 1°	SST, SSS, CHL*, DO100

* were not included in the GAM analysis.

Table 3. Top five candidate models selected by the dredge function of the “MuMIn” R-package. The model, predictor variable used, the degrees of freedom (DF), effective degrees of freedom (EDF), Akaike information criterion (AIC) value, and percentage of deviance explained. The ‘best’ model was selected based on the significance of predictor terms, the minimum value of AIC, and the maximum value of deviance explained.

Model	Predictor variable	Df/Edf	AIC	P-value	Dev. explained (%)
Year+Quarter+Flag+SST +SSS+MLD+DO100	Year	19	40022	< 0.001	62.1
	Quarter	3		< 0.001	
	Flag	20		< 0.001	
	SST	8.86		< 0.001	
	SSS	8.71		< 0.001	
	MLD	2.83		< 0.001	
	DO100	8.84	< 0.001		
Year+Quarter+Flag+SST +SSS+DO100	Year	19	40155	< 0.001	61.7
	Quarter	3		< 0.001	
	Flag	20		< 0.001	
	SST	8.87		< 0.001	
	SSS	7.88		< 0.001	
	DO100	7.92		< 0.001	
Quarter+Flag+SST+SSS +MLD+DO100	Quarter	3	40259	< 0.001	61.5
	Flag	20		< 0.001	
	SST	8.87		< 0.001	
	SSS	7.87		< 0.001	
	MLD	2.86		< 0.001	
	DO100	7.9		< 0.001	
Quarter+Flag+SST+SSS +DO100	Quarter	3	40419	< 0.001	61
	Flag	20		< 0.001	
	SST	8.87		< 0.001	
	SSS	7.88		< 0.001	
	DO100	7.92		< 0.001	
Year+Quarter+Flag+SST +MLD+DO100	Year	19	40911	< 0.001	59.9
	Quarter	3		< 0.001	
	Flag	20		< 0.001	
	SST	8.88		< 0.001	
	MLD	2.91		< 0.001	
	DO100	7.86		< 0.001	

Table 4. Percentage changes (denotes as Δ) in residual deviance and Akaike information criterion value of dropping each main effects factor from the GAM.

Variable	Δ Deviance (%)	Δ AIC (%)
Year	1.7	0.6
Quarter	5.6	2.3
Flag	21.5	8.2
SST	6.5	2.7
SSS	5.7	2.3
MLD	1.1	0.5
DO100	22.3	8.6

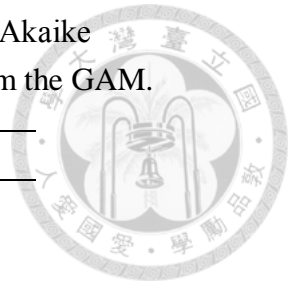
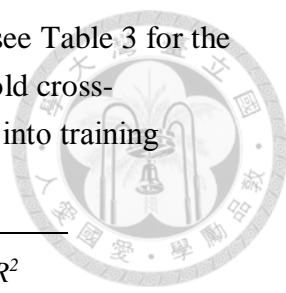


Table 5. Cross-validation results for the top five candidate models (see Table 3 for the model list). The average R^2 values were measured by using a five-fold cross-validation procedure in which input data were randomly partitioned into training (80%) and testing datasets (20%) for five model runs.



Model	Training R^2	Validation R^2
1	0.62 ± 0.01	0.61 ± 0.01
2	0.61 ± 0.01	0.60 ± 0.01
3	0.61 ± 0.01	0.60 ± 0.01
4	0.6 ± 0.01	0.60 ± 0.01
5	0.59 ± 0.01	0.59 ± 0.01

Figures

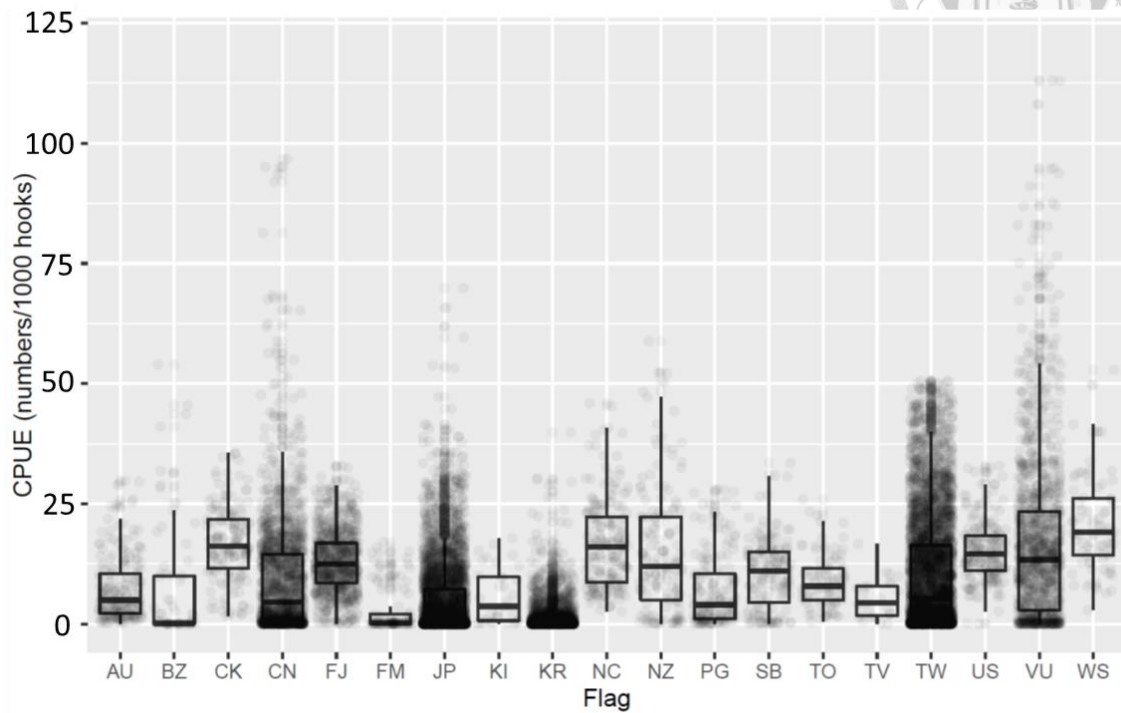
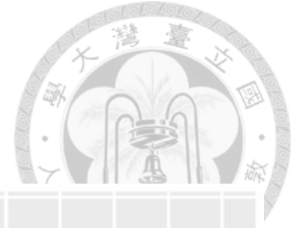


Figure 1. Boxplot of catch-per-unit-effort (CPUE, numbers/1000 hooks) of albacore overlaid on jitter data points by flags after the process of data grooming. Flag code was defined in Table 1.

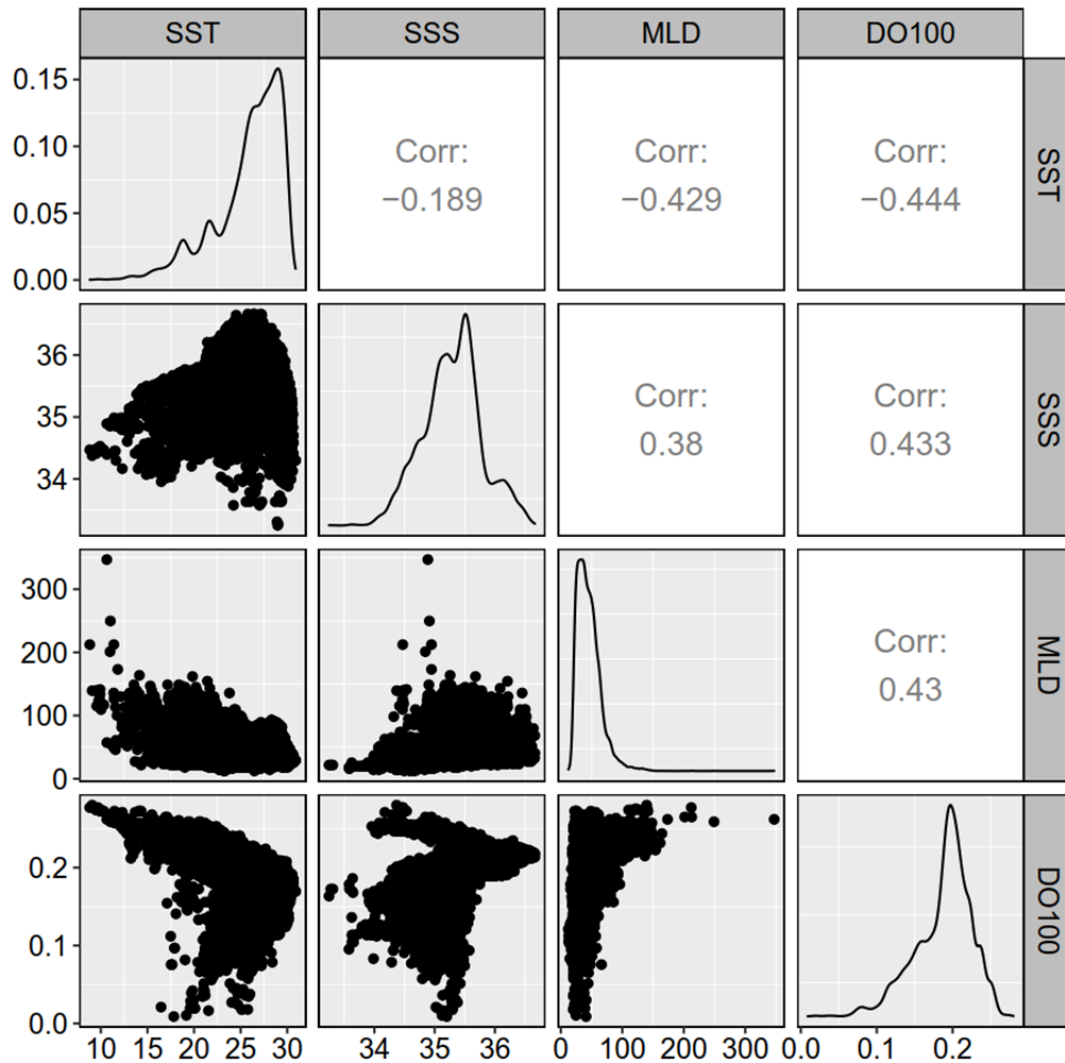


Figure 2. Pairwise scatter plots (lower triangle matrix) of environmental variables used in GAM analysis, including the sea surface temperature (SST, °C), sea surface salinity (SSS, PSU), mixed layer depth (MLD, m), and dissolved oxygen concentration under 100 m depth (DO100, mmol L⁻¹). The upper triangle matrix denotes the Pearson correlation coefficients. The diagonal axis denotes the density distributions of the environmental variables.

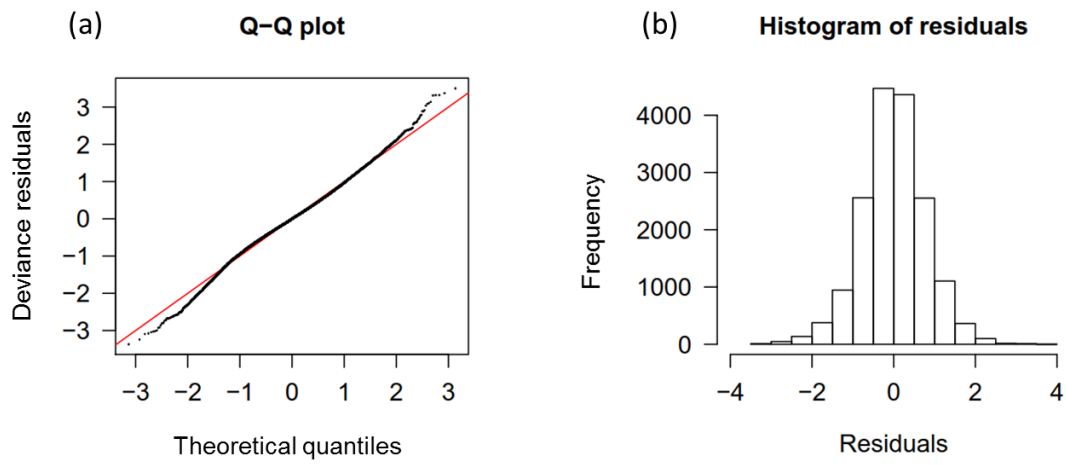


Figure 3. Residual diagnostics of (a) Normal Quantile-Quantile plot and (b) residual distribution plot of the GAM analysis.

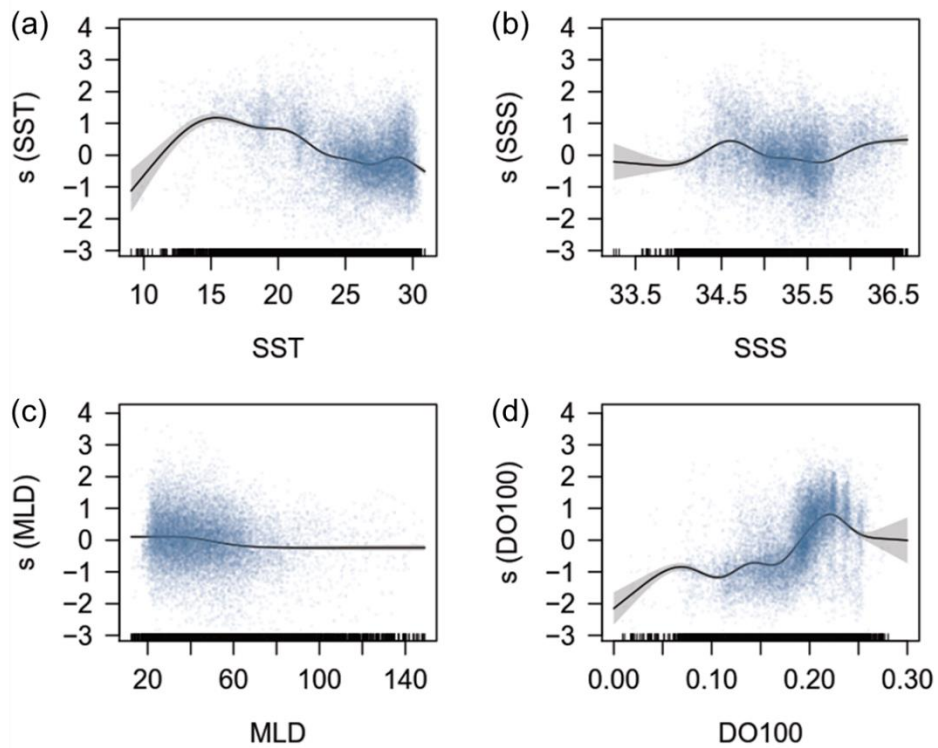


Figure 4. Response curves for the environmental variables, including the (a) sea surface temperature (SST, °C); (b) sea surface salinity (SSS, PSU); (c) mixed layer depth (MLD, m), and (d) dissolved oxygen concentration under 100m depth (DO100, mmol L^{-1}), derived from the GAM model. The blue points represent the partial residuals of observed CPUE data, and the gray polygons represent the 95% confidence interval. The hatch marks at the bottom are a descriptor of the frequency of data points.

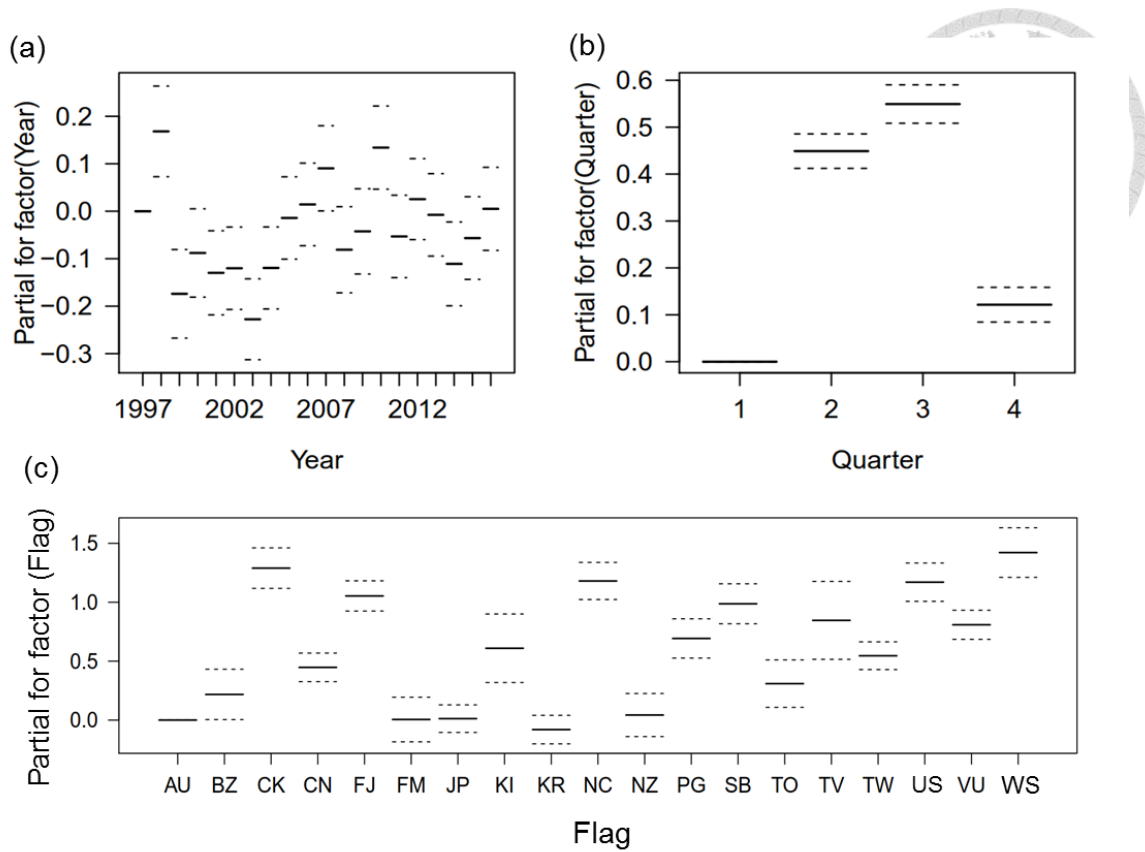


Figure 5. Response plots for (a) year, (b) quarter, and (c) flag factors derived from the GAM model. The dashed lines denote the 95% confidence interval. Flag code was defined in Table 1.

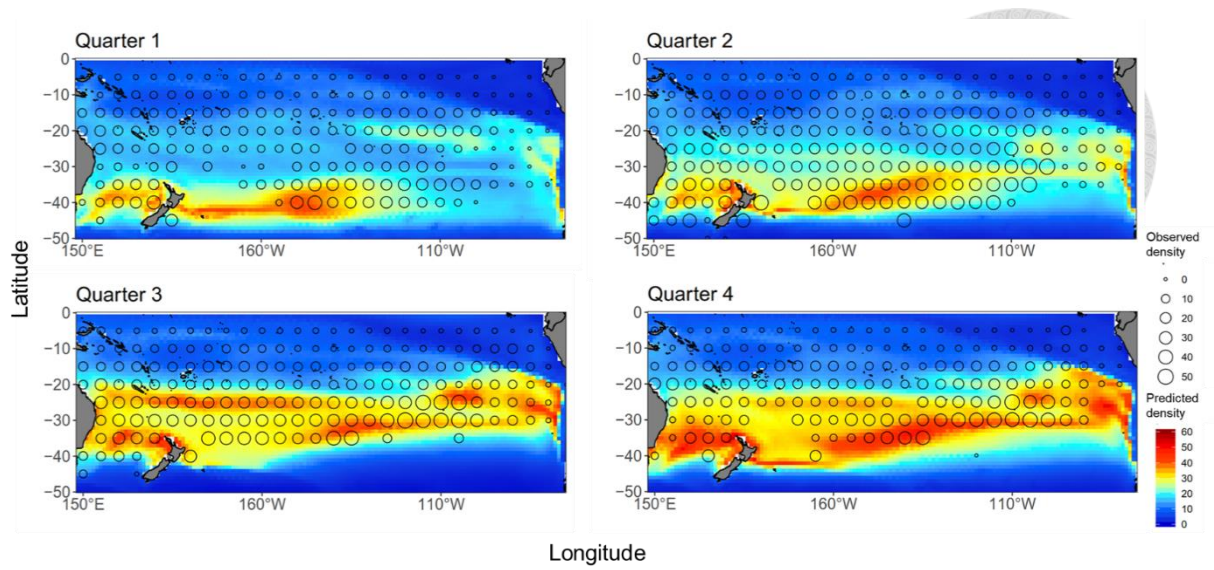


Figure 6. Quarterly average catch-per-unit-effort (CPUE) (number/1,000 hooks) distributions (open circles) for the south Pacific albacore overlaid on the median-ensemble density map (color contours) based on the GAM which was developed with data from 1997 to 2016.

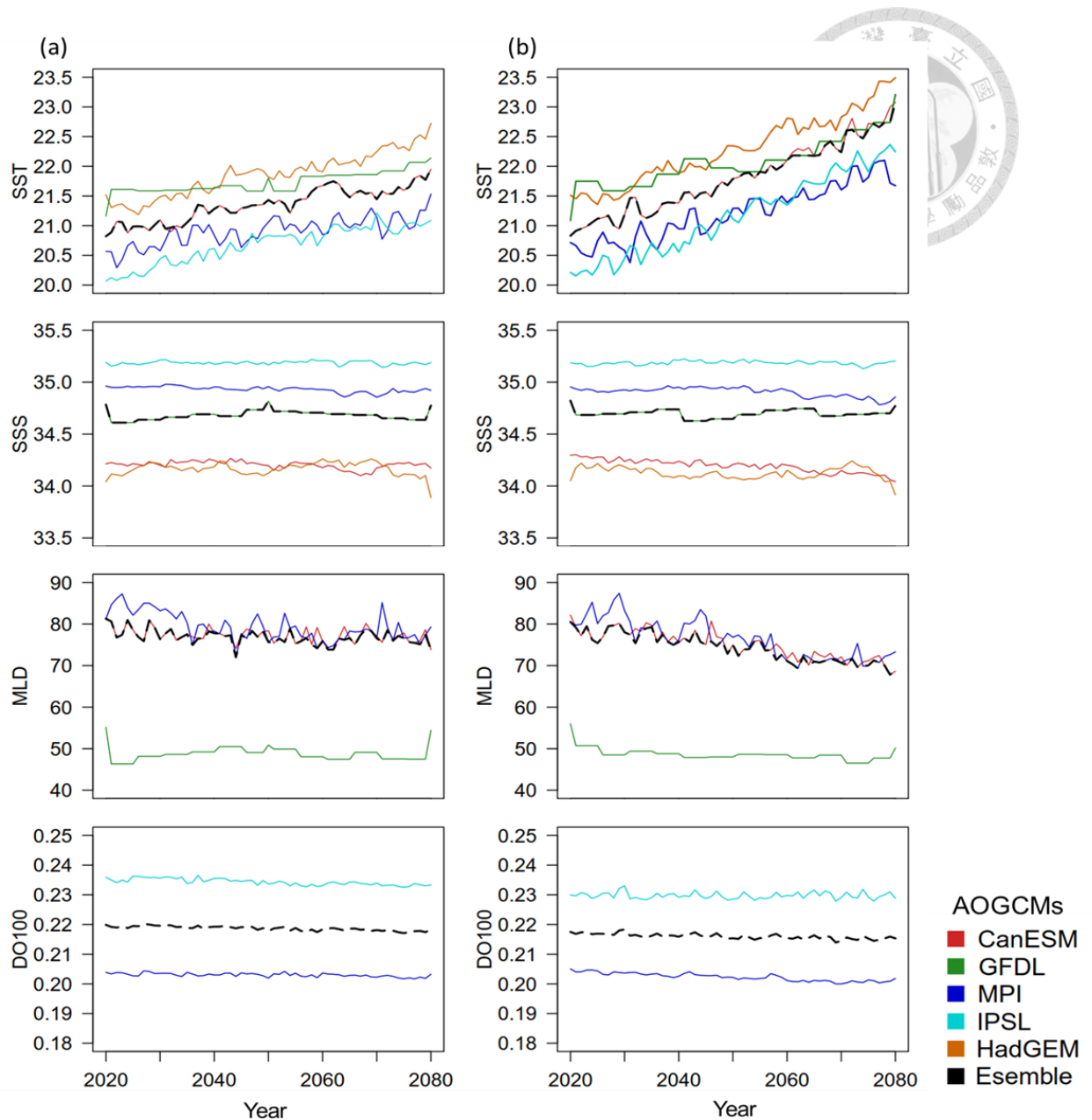


Figure 7. Annual time-series of the areal-averaged environmental variables, including the sea surface temperature (SST, °C); sea surface salinity (SSS, PSU); mixed layer depth (MLD, m), and dissolved oxygen concentration under 100m depth (DO100, mmol L⁻¹), derived from IPCC atmosphere-ocean general circulation models (AOGCMs) (see Table 2 for model names) from 2020 to 280 under the (a) RCP4.5 and (b) RCP8.5 scenarios. DO100 were only available for the IPSL and MPI. Solid color lines denote the AOGCMs. Black dash line denotes the median-ensemble result.

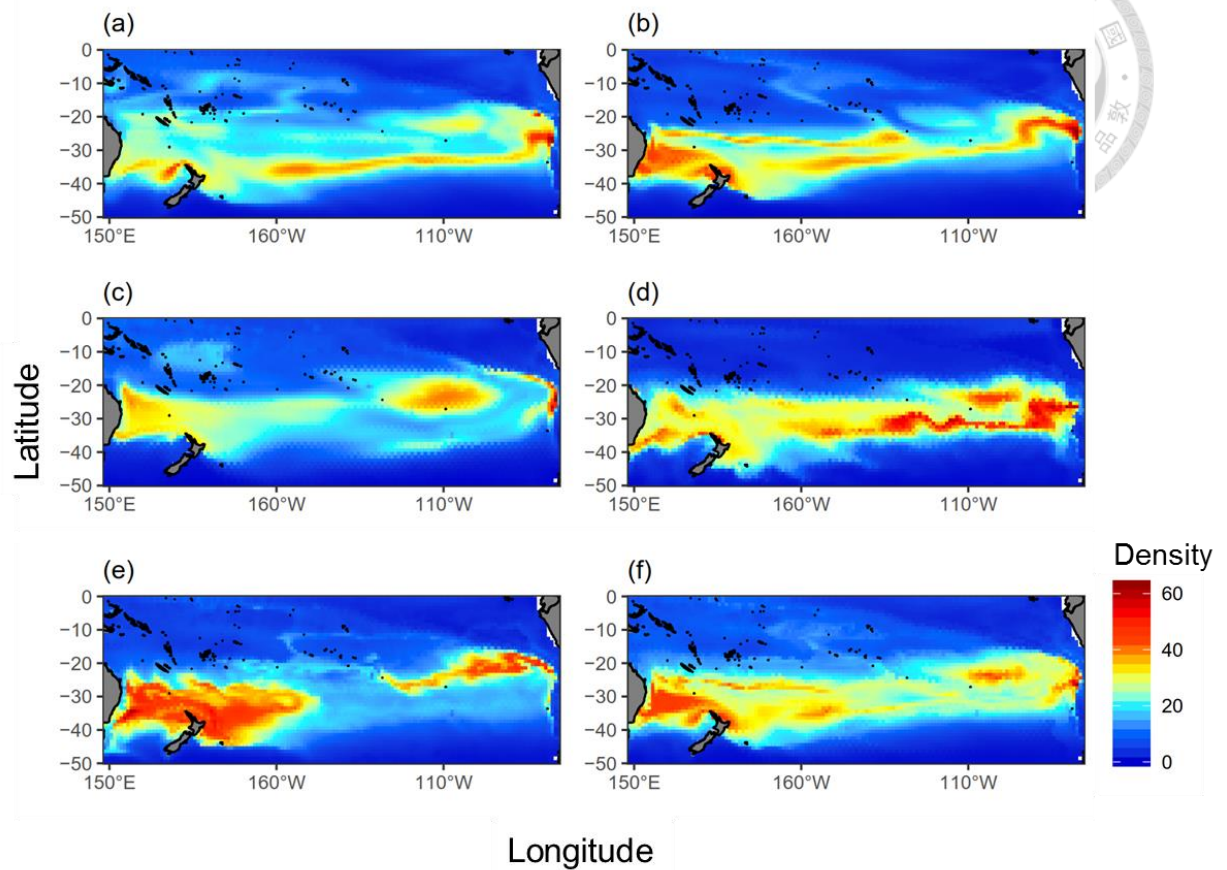


Figure 8. Spatial distributions of the predicted albacore density (number/1,000 hooks) in quarter 3 of 2020 derived from the atmosphere-ocean general circulation models (AOGCMs) of (a) GFDL; (b) CanESM; (c) IPSL; (d) MPI; and (e) HadGEM under the RCP4.5 scenario. The median-ensemble prediction estimated from the five AOGCMs was shown in (f).

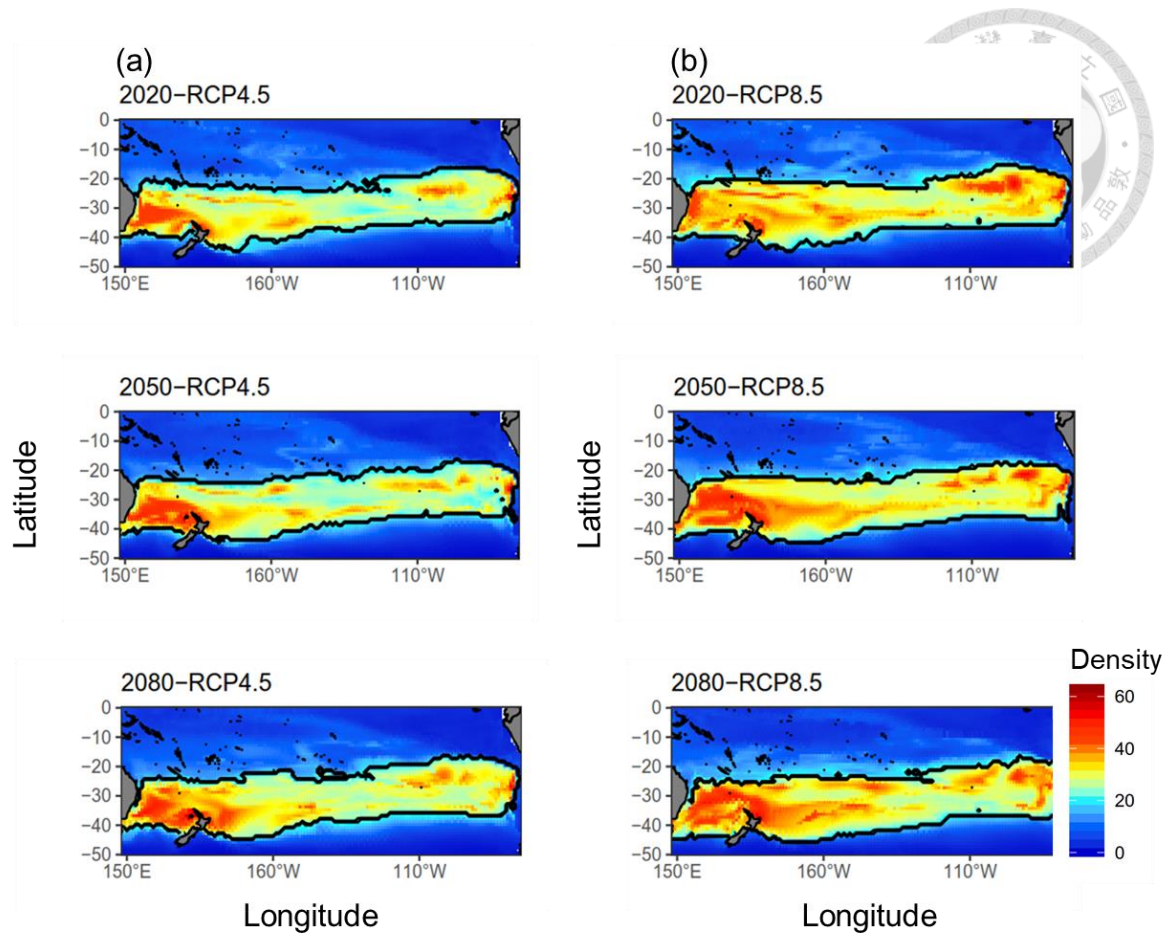


Figure 9. The future ensemble projections of south Pacific albacore density (number/1,000 hooks) distributions in quarter 3 estimated from the five atmosphere-ocean general circulation models (AOGCMs) for the current (2020), mid (2050), and late (2080) periods of the 21st century under the (a) RCP4.5 and (b) RCP8.5 (right panel) scenarios. The solid black lines denote the preferred habitat boundaries defined by density >25 number/1,000 hooks.

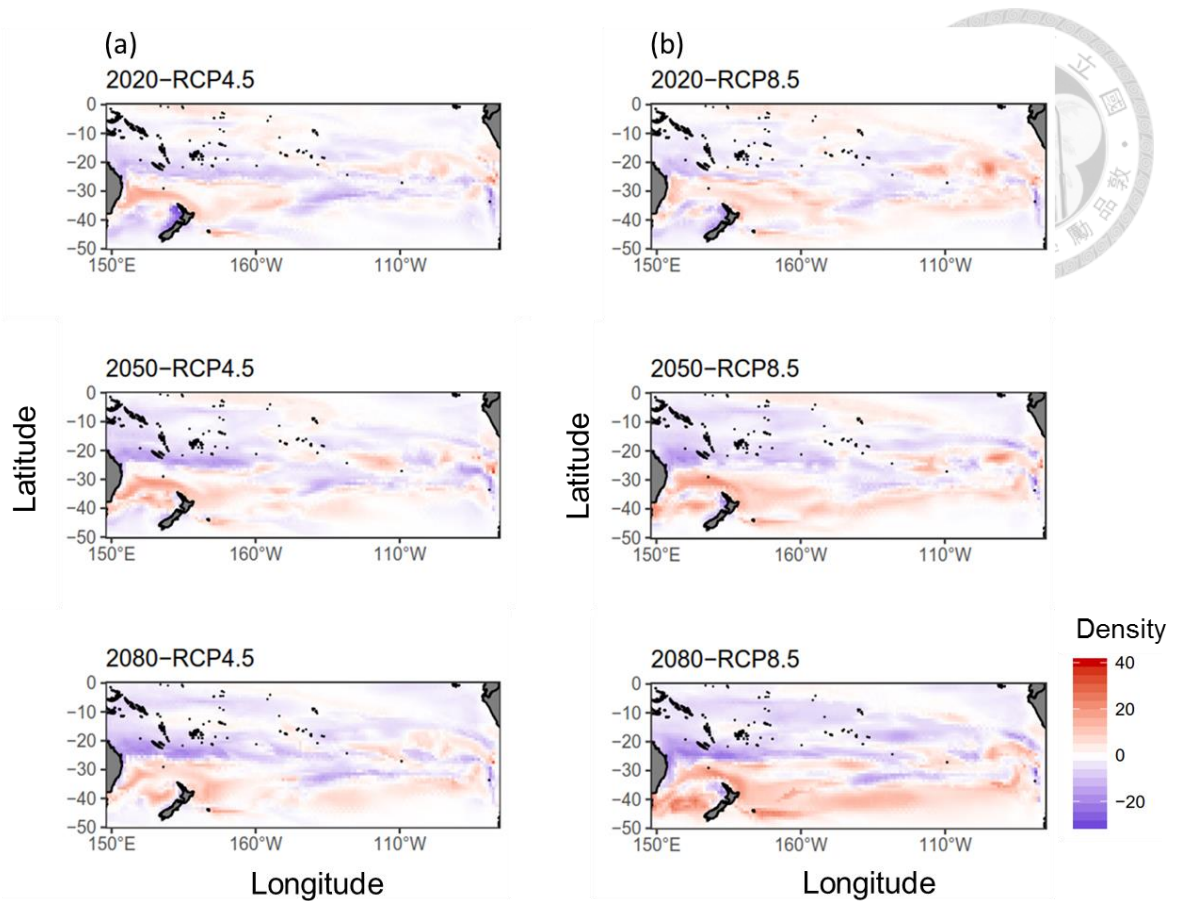


Figure 10. The spatial distributions of density (number/1,000 hooks) anomalies of south Pacific albacore in quarter 3 calculated by subtracting the predictions of the median ensemble GAM projections in 2020, 2050, and 2080 from the recent average of 2012-2016 under the (a) RCP4.5 and (b) RCP8.5 scenarios.

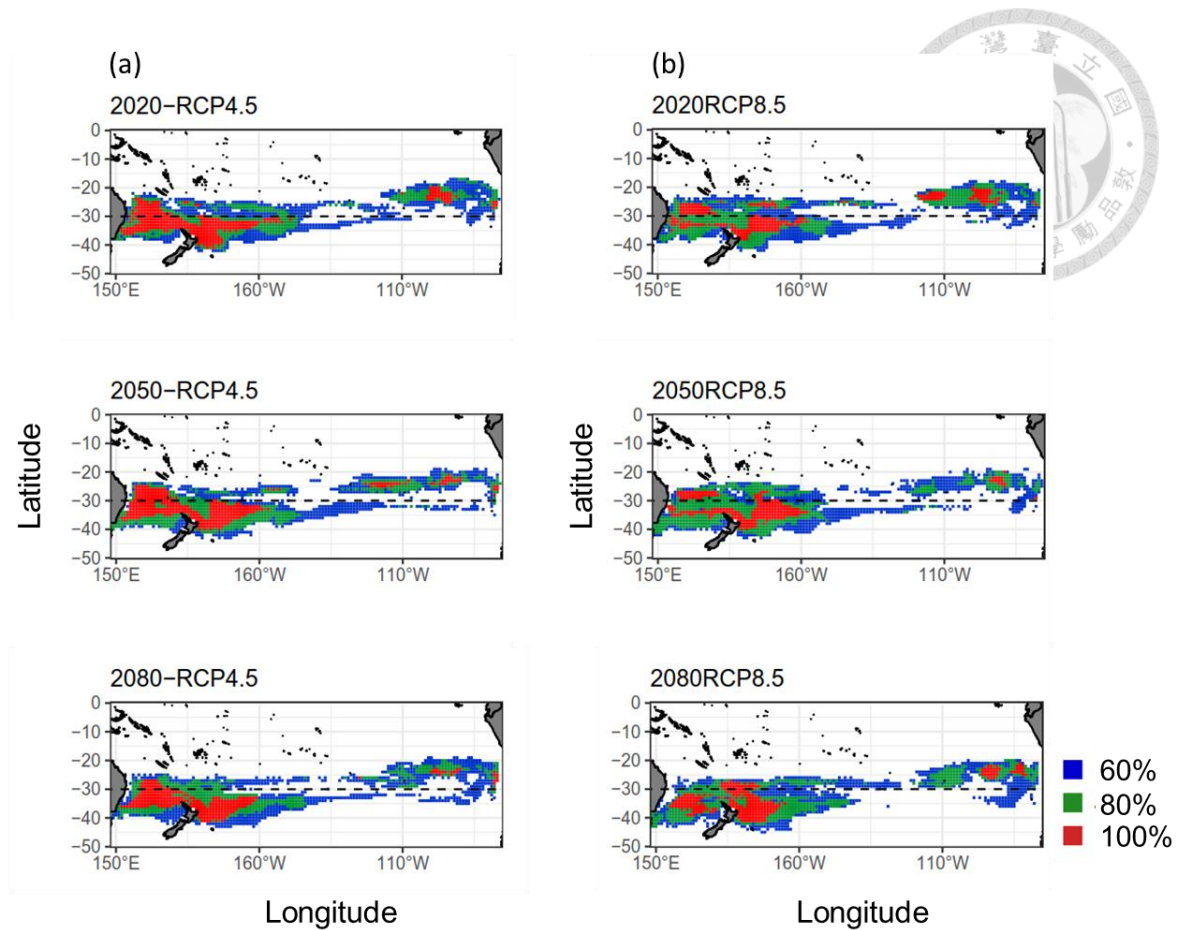


Figure 11. Ensemble agreement maps of the south Pacific albacore habitat predictions by five atmosphere-ocean general circulation models (AOGCMs) for the current (2020), mid (2050), and late (2080) periods of the 21st century under the (a) RCP4.5 and (b) RCP8.5 (right panel) scenarios. Colors denote the probabilities of habitat map based on the levels of agreement among five AOGCMs.

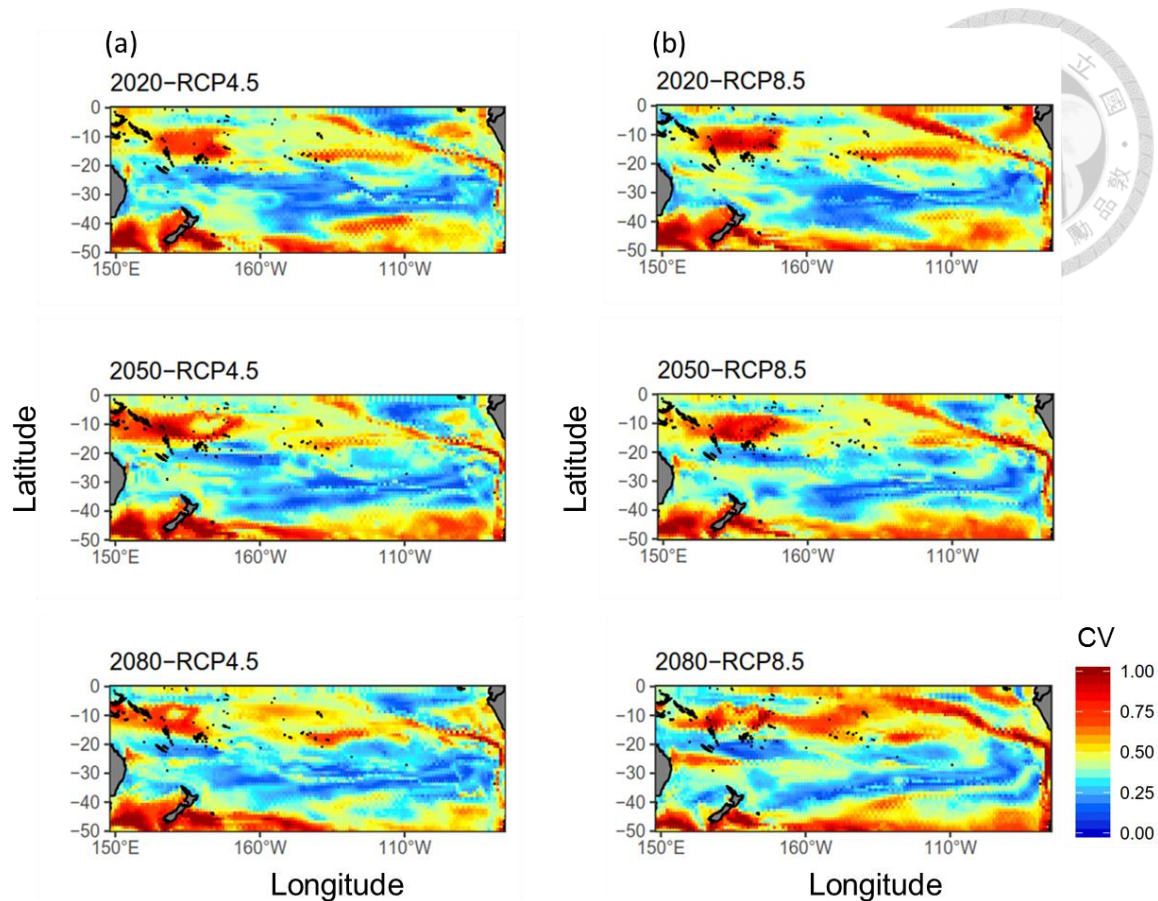


Figure 12. Spatial distributions of the uncertainty (measured by the coefficient of variance, CV) of predicted density (number/1,000 hooks) of south Pacific albacore in quarter 3 estimated from the five atmosphere-ocean general circulation models (AOGCMs) for the current (2020), mid (2050), and late (2080) periods of the 21st century under the (a) RCP4.5 and (b) RCP8.5 scenarios.

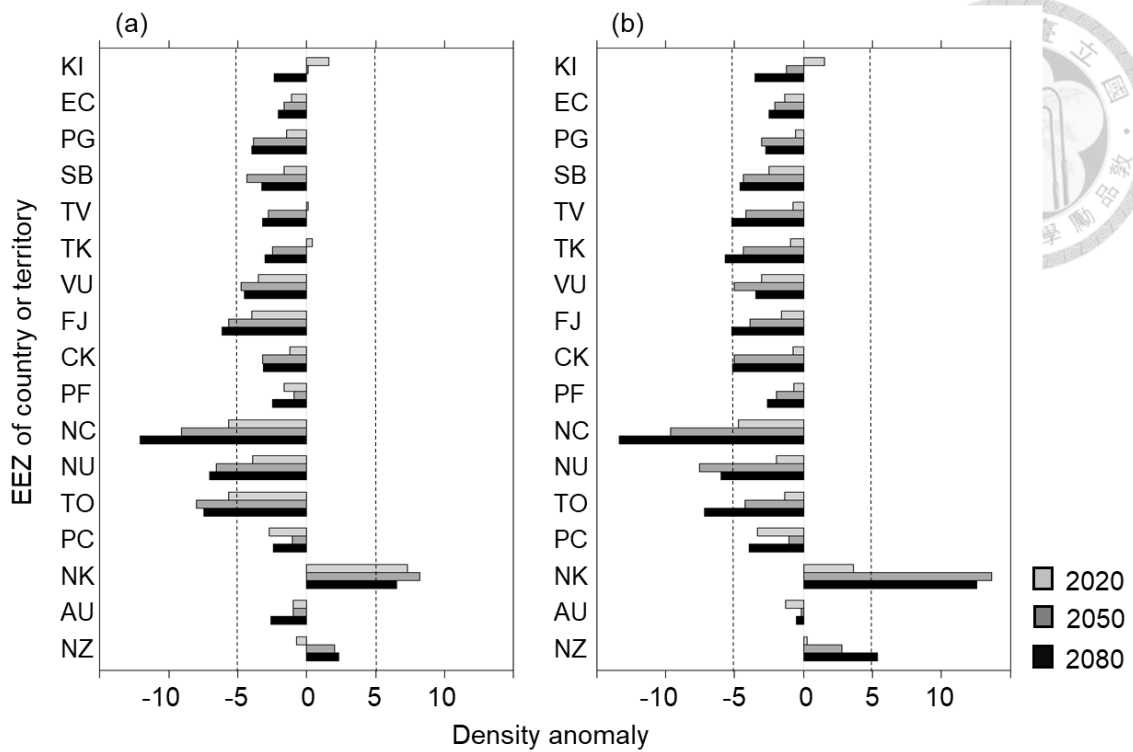
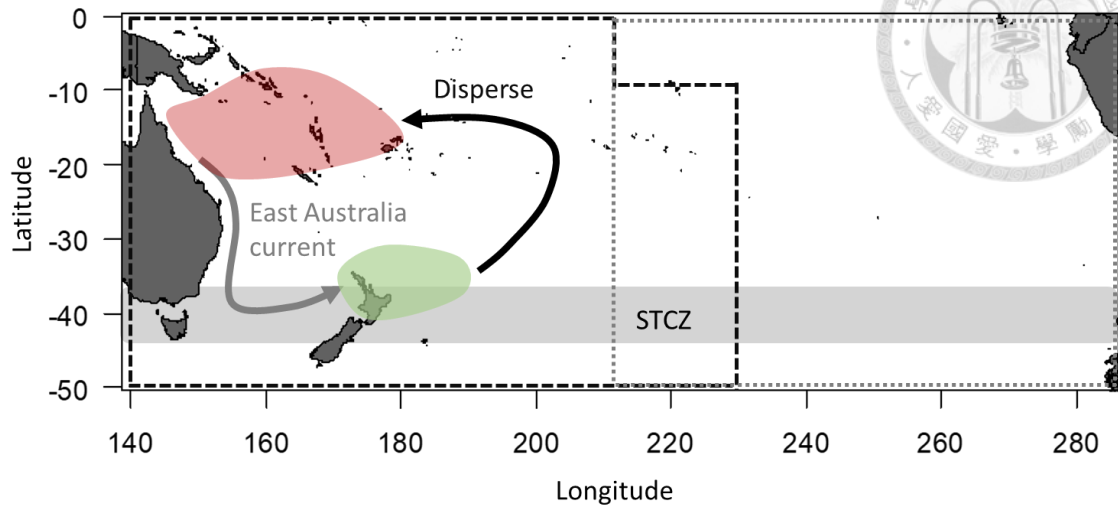
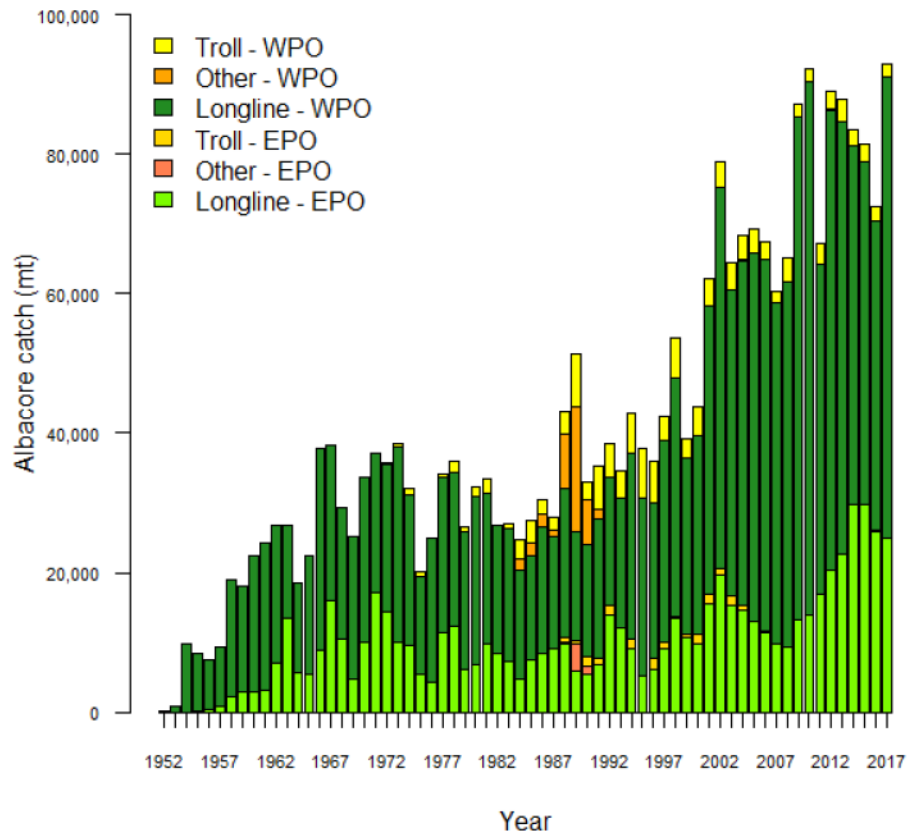


Figure 13. Changes in albacore density (number/1,000 hooks) within the exclusive economic zones (EEZs) of the countries or territories in the south Pacific Ocean for the current (2020), mid (2050), and late (2080) periods of the 21st century relative to 2012-2016 under the (a) RCP4.5 and (b) RCP8.5 scenarios. Only those countries or territories that had more than 30% of fishery data inside their EEZs were analyzed in this study. Countries or territories were ordered per mean latitude of the EEZ. The vertical dashed lines denote the reference line of ± 5 density anomalies. Country codes not shown in table 1 were illustrated below. EC, Galapagos Islands; TK, Tokelau; NU, Niue; PC, Pitcairn; NK, Norfolk Island.

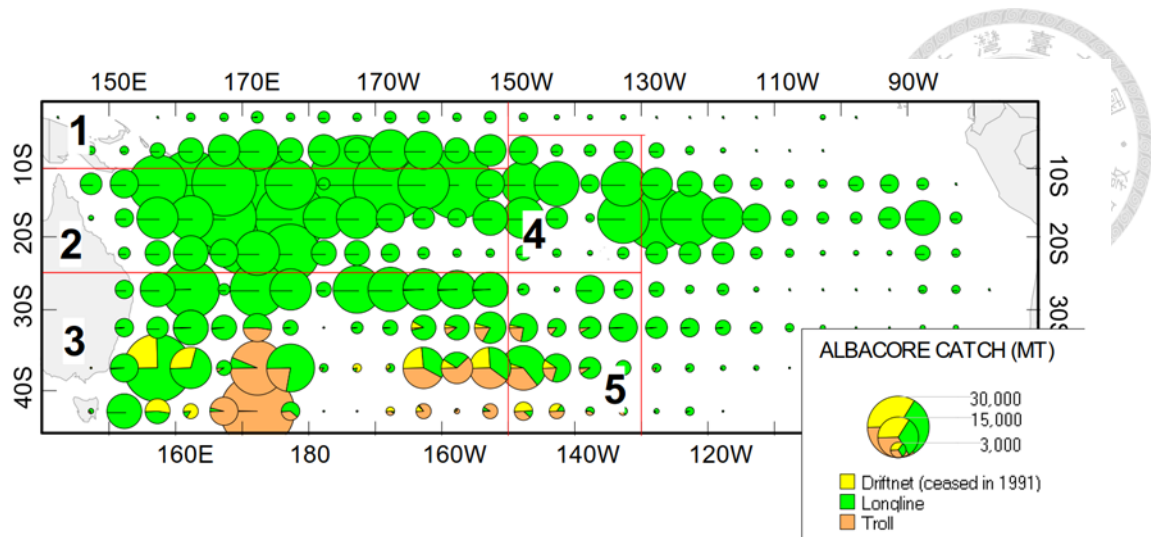
Appendix Figures



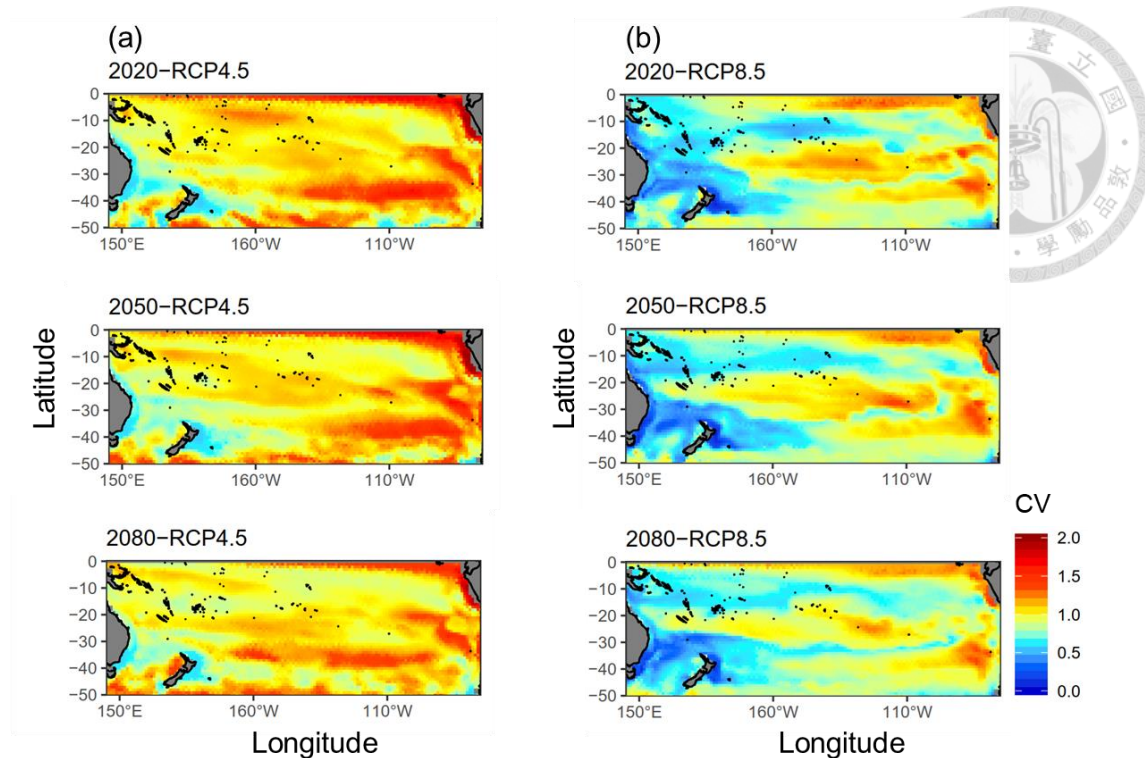
Appendix figure 1. Map of schematic seasonal migration route of the albacore in the Western and Central Pacific Ocean. Mature albacore (> 80 cm fork length) migrates to spawning ground (the Coral Sea, red polygon) during late spring and early summer. Larvae and juveniles hatch around the spawning ground and are transported along the East Australia Current (grey line) to the feeding ground in the coastal waters off New Zealand (green polygon) during late summer and fall. Juveniles (< 80 cm fork length) disperse northwards (black line) from the Subtropical Convergence Zone (STCZ, grey polygon) during late fall and winter. The broken black line denotes the WCPFC convention area, the dotted grey line denotes the IATTC convention area.



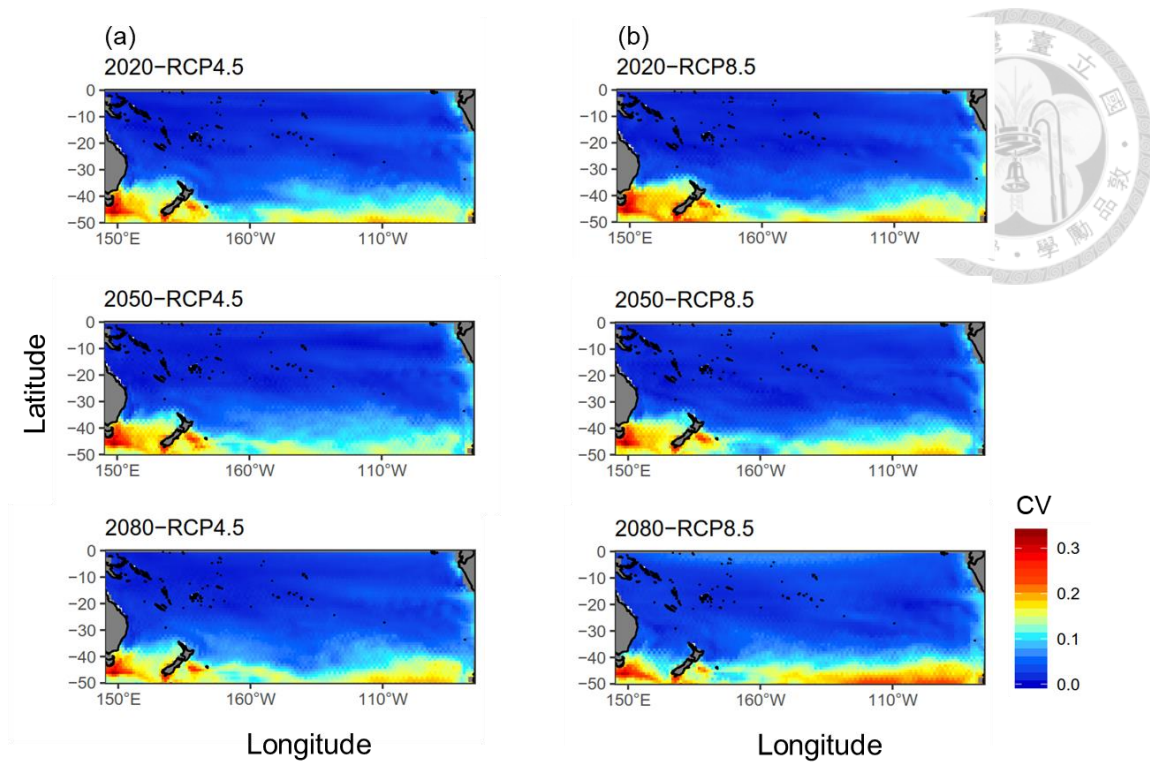
Appendix figure 2. Time-series of total annual catches of South Pacific albacore (in metric ton) by fishing gears. WPO represents the western Pacific Ocean; EPO represents the eastern Pacific Ocean (source: WCPFC-SC14-2018/ SA-IP-08 Rev. 2).



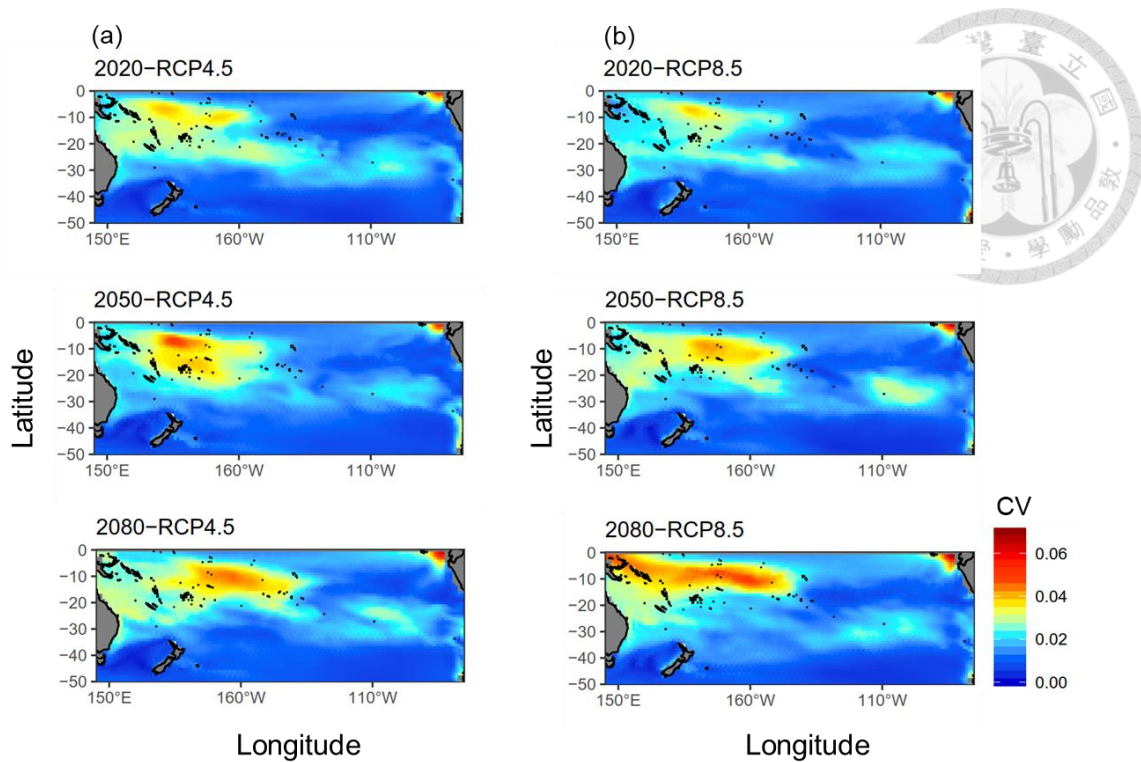
Appendix figure 3. Spatial distribution of south Pacific albacore catches by fisheries during 1988 - 2018. Colors denote gear types. The red lines indicate the five-region spatial stratification used in the stock assessment. (source: WCPFC-SC15-2019/GN WP-1).



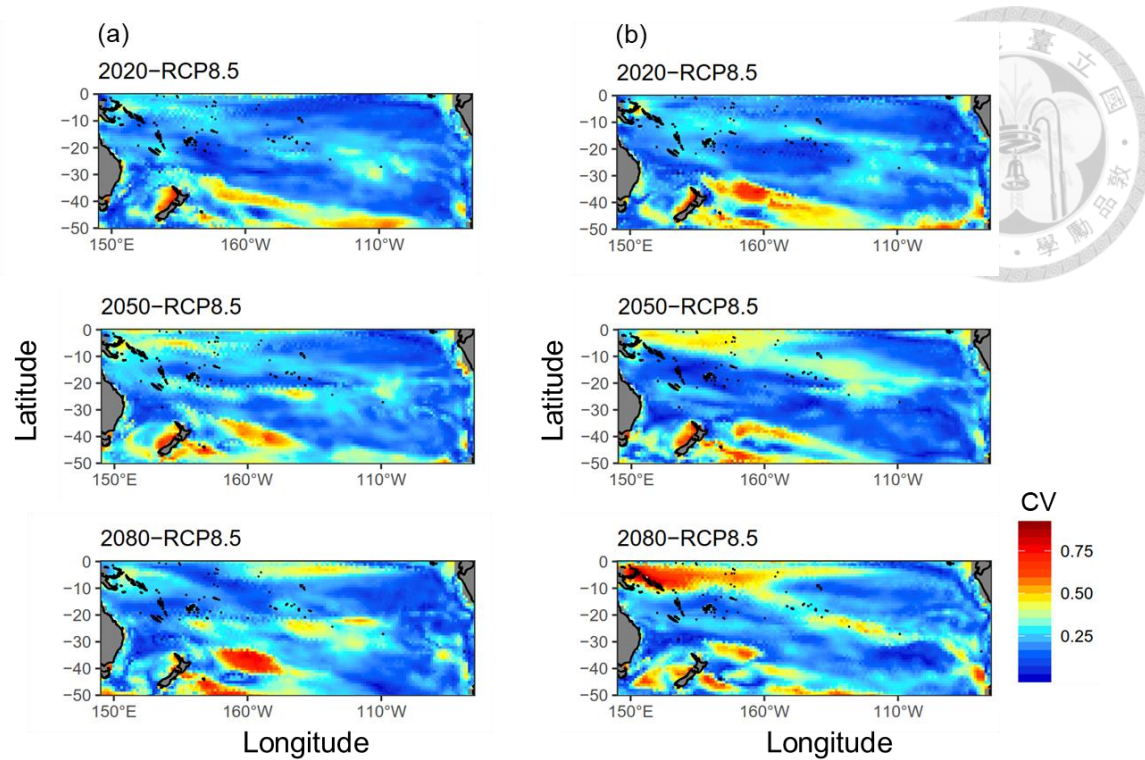
Appendix figure 4. Spatial distributions of the uncertainty (measured by the coefficient of variance, CV) of the projected chlorophyll-a concentration estimated across five atmosphere-ocean general circulation models for the current (2020), mid (2050), and late (2080) periods of the 21st century under the (a) RCP4.5 and (b) RCP8.5 scenarios.



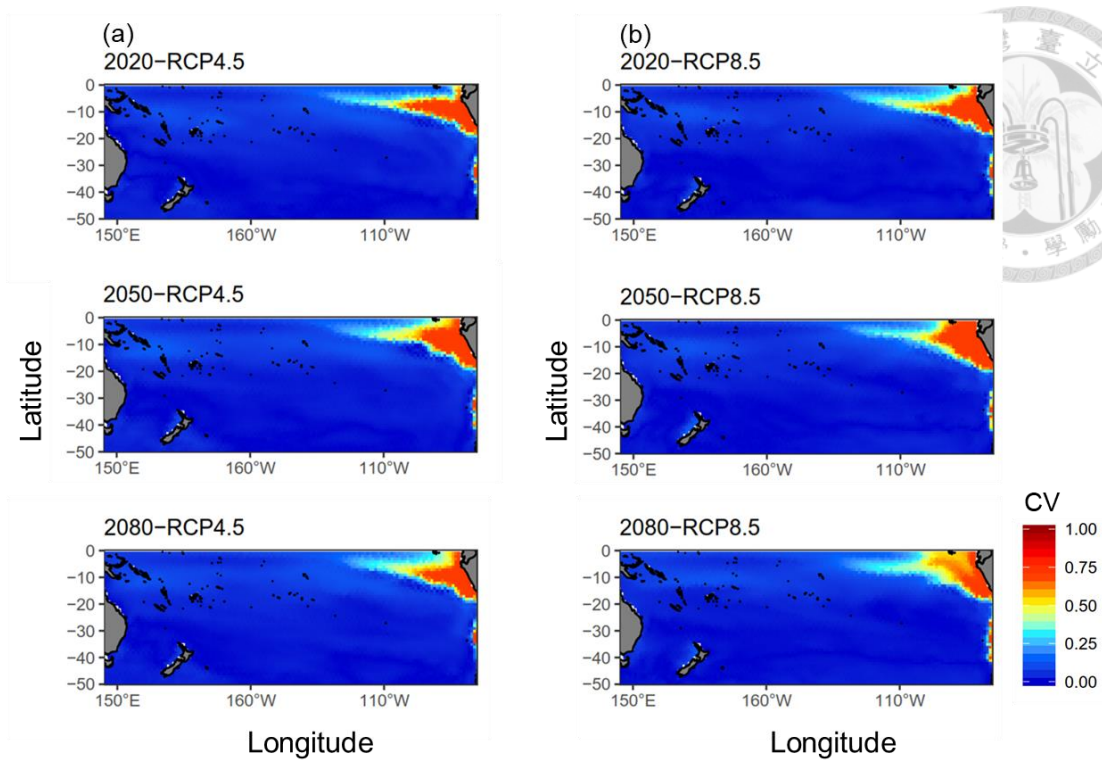
Appendix figure 5. Spatial distributions of the uncertainty (measured by the coefficient of variance, CV) of the projected sea surface temperature estimated across five atmosphere-ocean general circulation models for the current (2020), mid (2050), and late (2080) periods of the 21st century under the (a) RCP4.5 and (b) RCP8.5 scenarios.



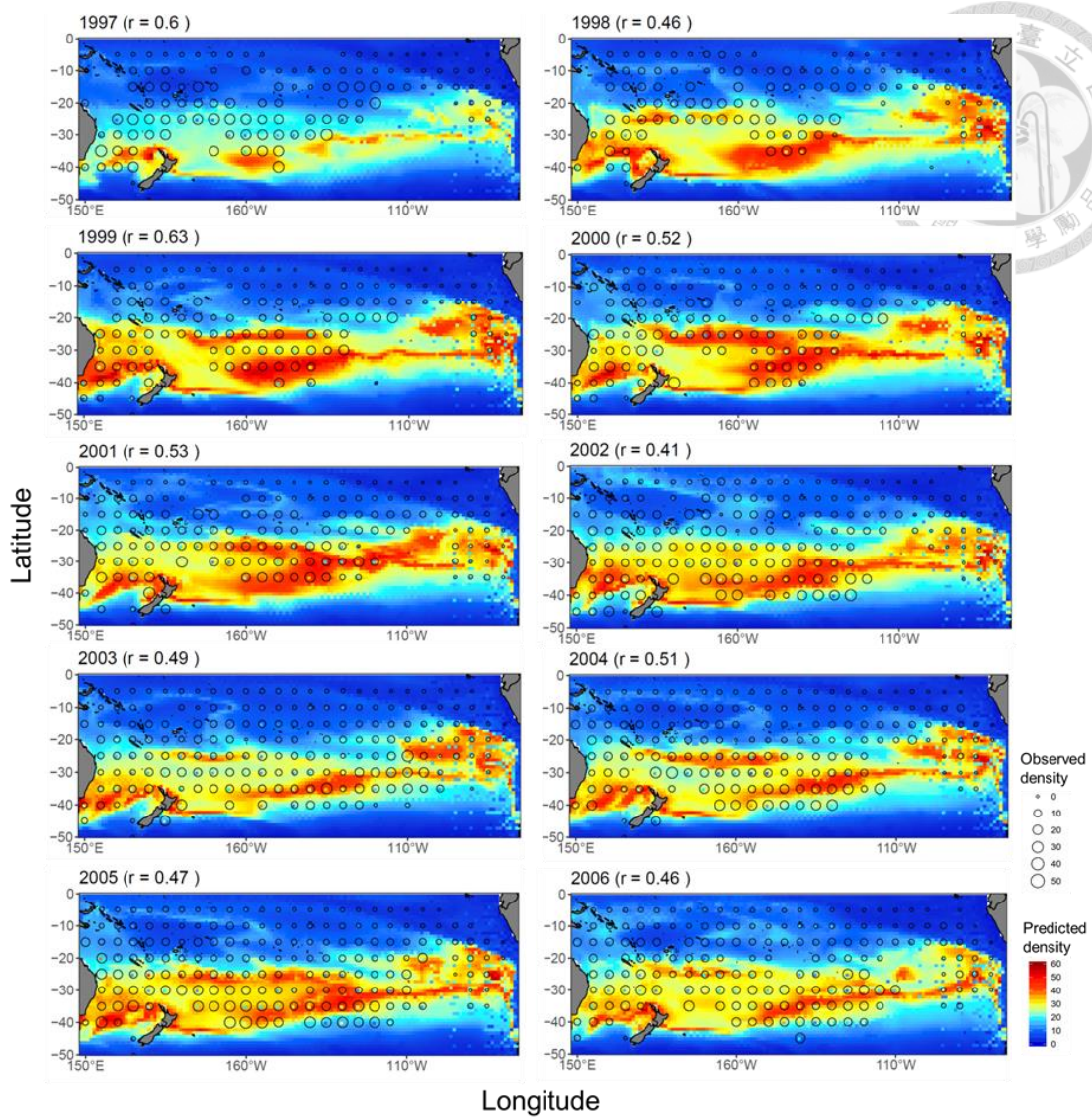
Appendix figure 6. Spatial distributions of the uncertainty (measured by the coefficient of variance, CV) of the projected sea surface salinity estimated across five atmosphere-ocean general circulation models for the current (2020), mid (2050), and late (2080) periods of the 21st century under the (a) RCP4.5 and (b) RCP8.5 scenarios.



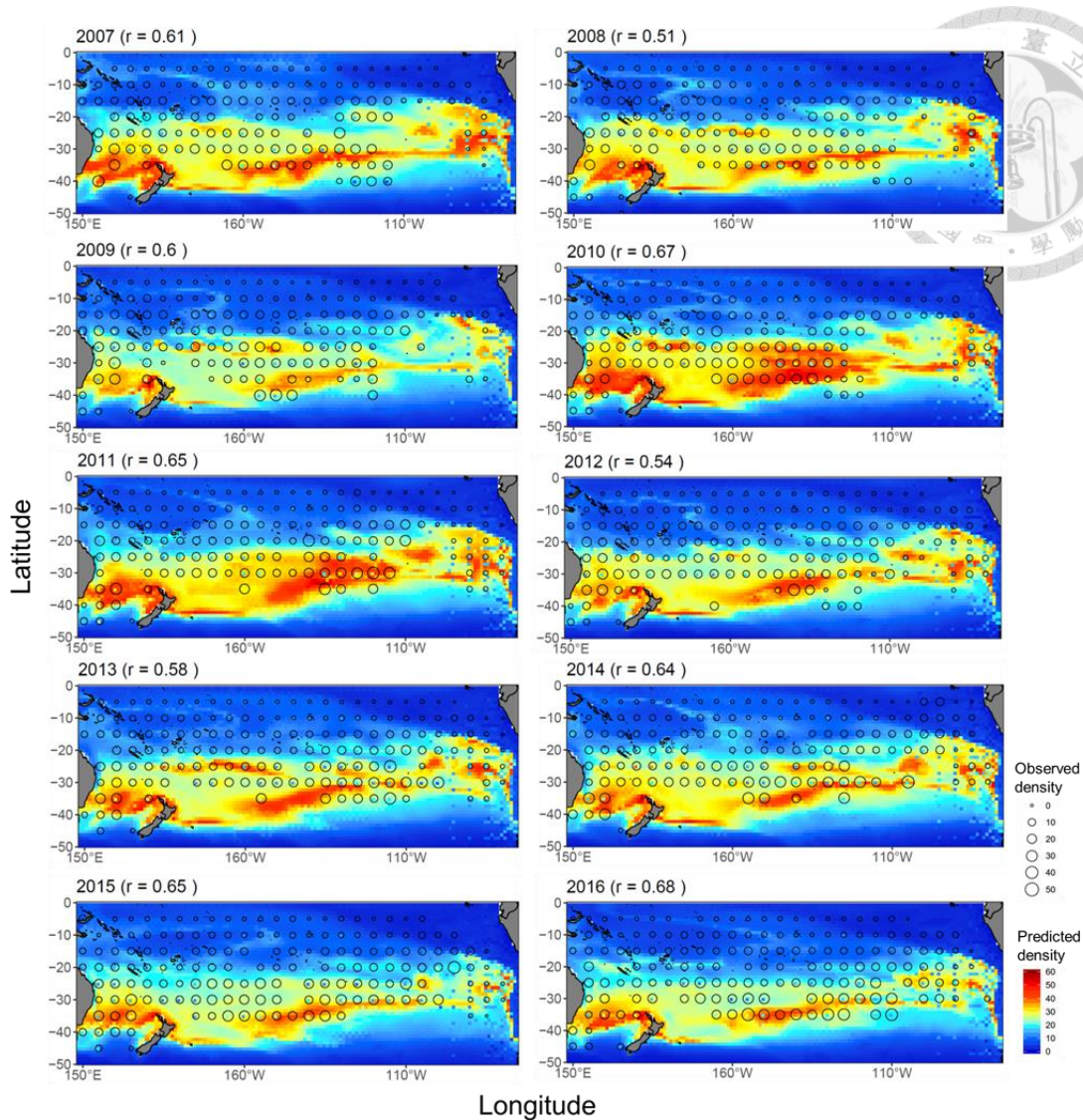
Appendix figure 7. Spatial distributions of the uncertainty (measured by the coefficient of variance, CV) of the projected mixed layer depth estimated across five atmosphere-ocean general circulation models for the current (2020), mid (2050), and late (2080) periods of the 21st century under the (a) RCP4.5 and (b) RCP8.5 scenarios.



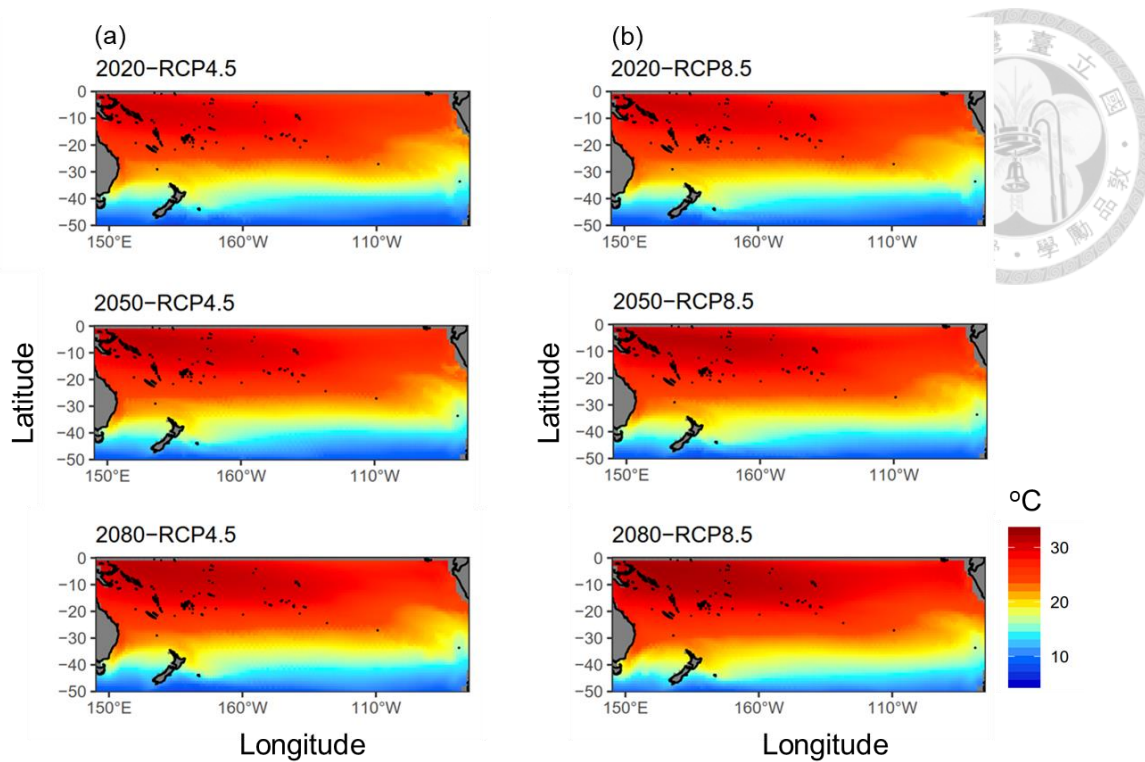
Appendix figure 8. Spatial distributions of the uncertainty (measured by the coefficient of variance, CV) of the projected dissolved oxygen estimated across five atmosphere-ocean general circulation models for the current (2020), mid (2050), and late (2080) periods of the 21st century under the (a) RCP4.5 and (b) RCP8.5 scenarios.



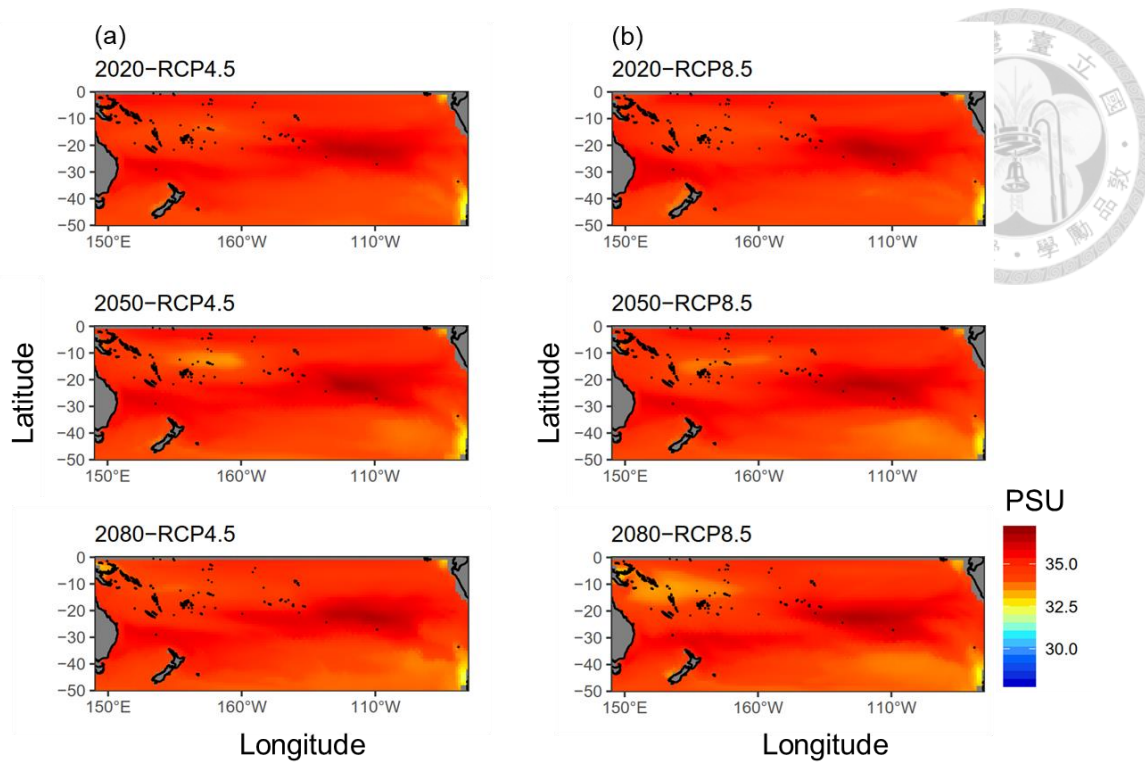
Appendix figure 9. Annual catch-per-unit-effort (CPUE) (number/1,000 hooks) distributions (open circles) for the south Pacific albacore overlaid on the median-ensemble density map (color contours) in 1997 - 2006 based on the GAM which was developed with data from 1997 to 2016, Pearson correlation coefficients (r) of predicted and observed values were shown for each year.



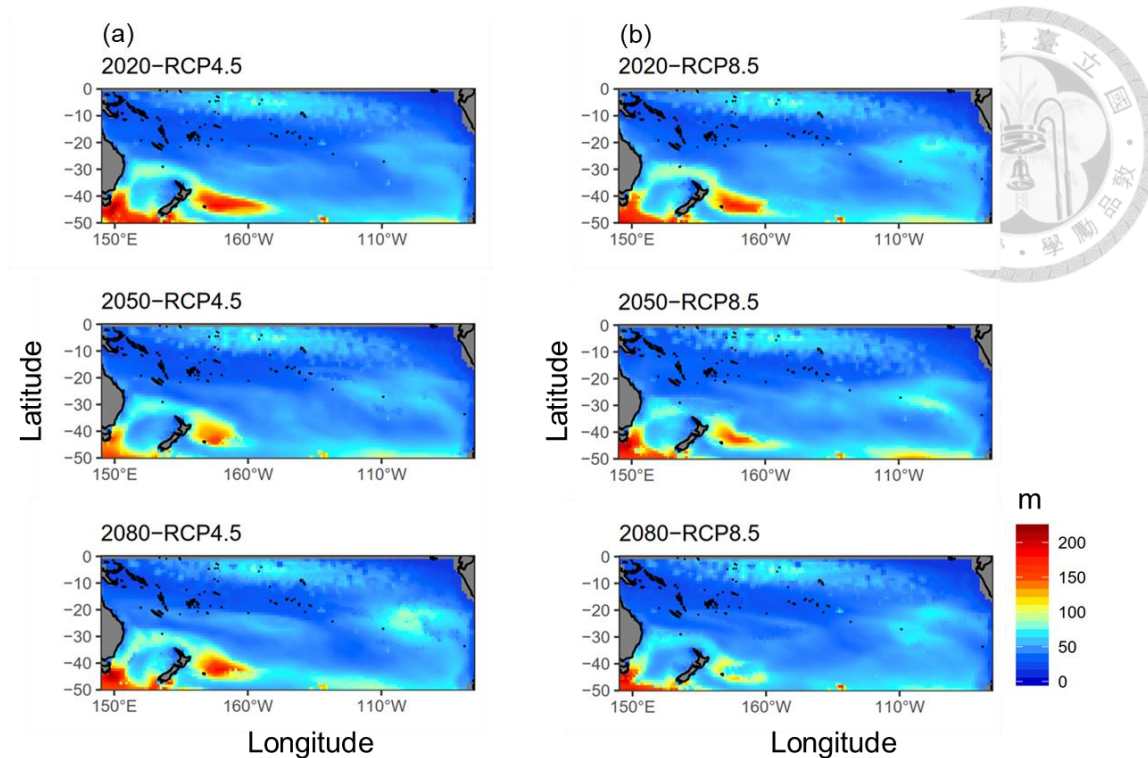
Appendix figure 10. Annual catch-per-unit-effort (CPUE) (number/1,000 hooks) distributions (open circles) for the south Pacific albacore overlaid on the median-ensemble density map (color contours) in 2007 - 2016 based on the GAM which was developed with data from 1997 to 2016, Pearson correlation coefficients (r) of predicted and observed values were shown for each year.



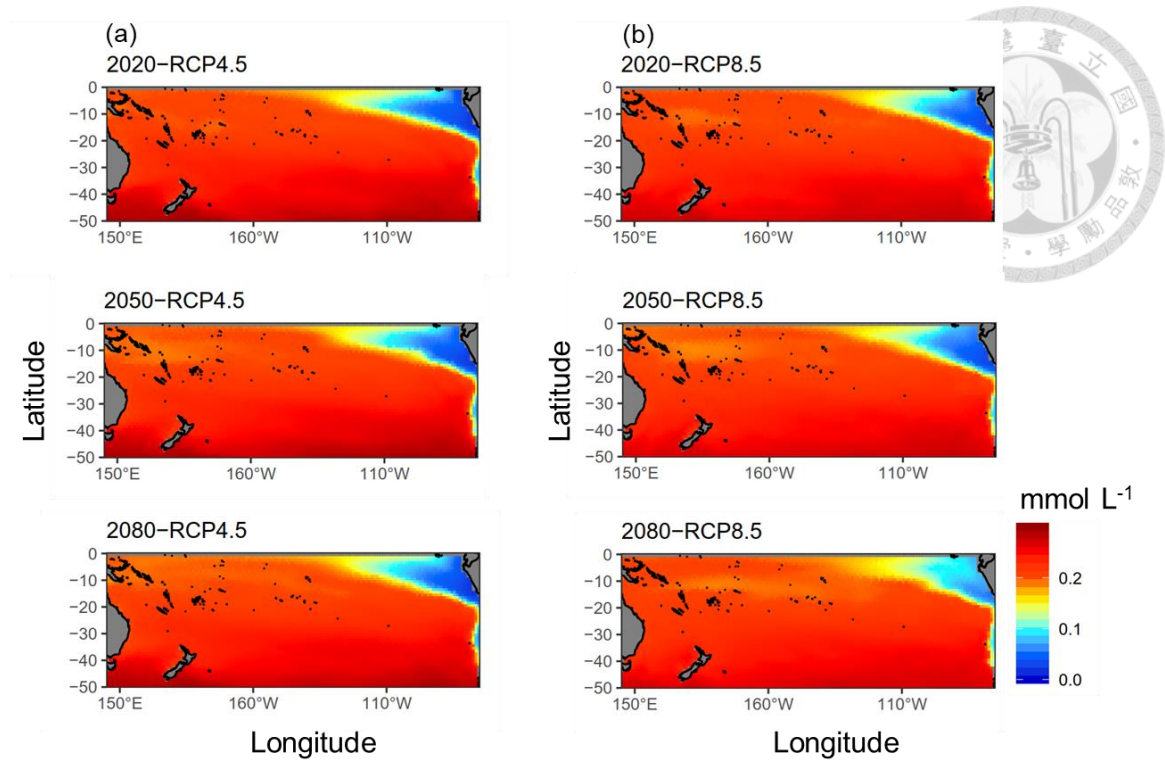
Appendix figure 11. Median-ensemble maps of the projected sea surface temperature derived from five atmosphere-ocean general circulation models for the current (2020), mid (2050), and late (2080) periods of the 21st century under the (a) RCP4.5 and (b) RCP8.5 scenarios



Appendix figure 12. Median-ensemble maps of the projected sea surface salinity derived from five atmosphere-ocean general circulation models for the current (2020), mid (2050), and late (2080) periods of the 21st century under the (a) RCP4.5 and (b) RCP8.5 scenarios.



Appendix figure 13. Median-ensemble maps of the projected mixed layer depth derived from five atmosphere-ocean general circulation models for the current (2020), mid (2050), and late (2080) periods of the 21st century under the (a) RCP4.5 and (b) RCP8.5 scenarios.



Appendix figure 14. Median-ensemble maps of the projected dissolved oxygen derived from five atmosphere-ocean general circulation models for the current (2020), mid (2050), and late (2080) periods of the 21st century under the (a) RCP4.5 and (b) RCP8.5 scenarios.